

DEVELOPMENT OF POLYURETHANE/CLAY NANOCOMPOSITES BASED ON PALM OIL POLYOL

Ummi Habibah^{1*}, Adriana¹, S Sariadi¹, Muhammad², Halim Zaini¹, Sabila Yasara SA¹, Fachraniah¹

¹Jurusan Teknik Kimia, Politeknik Negeri Lhokseumawe, Jl. Medan - Banda Aceh No.Km. 280, RW.Buketrata, Mesjid Punteut, Blang Mangat, Kota Lhokseumawe, Aceh 24301

²Jurusan Teknik Elektro, Universitas Malikussaleh, Jl. Batam, Blang Pulo, Kec. Muara Satu, Kota Lhokseumawe, Aceh 24355

*E-mail:ummihabibah@pnl.ac.id

ABSTRACT

Polyurethanes (PURs) are highly adaptable polymeric substances with a variety of physical and chemical attributes. High abrasion resistance, tear strength, shock absorption, flexibility, and elasticity are just a few of the desirable qualities of PURs. Despite their generally low thermal stability, this can be enhanced by utilizing clay that has been treated. From renewable resources, polyurethane/clay nanocomposites have been created. By combining oleic acid from palm oil with glycerol, a polyol for the manufacture of polyurethane by reaction with an isocyanate was created. As a catalyst and emulsifier, dodecylbenzene sulfonic acid (DBSA) was employed. Octadodecylamine (ODA-mont) and cetyltrimethyl ammonium bromide (CTAB-mont) were used to treat the unaltered clay (kunipia-F). The d-spacing in CTAB-mont and ODA-mont were bigger than that of the pure-mont (1.142 nm) at 1.571 nm and 1.798 nm, respectively. A pre-polymer technique was used to create polyurethane/clay nanocomposites, and the micro-domain structures of segmented PU, CTAB-mont-PU 1, 3, and 5 wt%, and ODA-mont-PU 1, 3, and 5 wt% were determined by FTIR spectra. X-ray diffraction (X-RD) was used to evaluate the nanocomposites' morphology, and the results revealed that all of the intercalated type's nanocomposites were created as a result of this effort. When the surfaces of the materials were examined using transmission electron microscopy (TEM) observation and scanning electron microscopy (SEM), these were further confirmed. Thermogravimetric analysis (TGA) was used to examine thermal stability. Pure PU begins to degrade around 200°C, which is lower than the degrading rates of CTAB-mont PU and ODA-mont PU, which occur at roughly 318°C and 330°C, respectively. Both pure polyurethane (PU) and PU/clay nanocomposites have their mechanical properties, including dynamic mechanical properties, tested. With only a 5 weight percent addition of the montmorillonite CTAB-mont PU or ODA-mont PU, respectively, the tensile strength of the nanocomposites increased by more than 214% and 267%, respectively, demonstrating the impressively positive impact of the modified organoclay on the strength and elongation at break of the nanocomposites.

Keywords: *Clay, Palm Oil, Polyurethane*

INTRODUCTION

Manufacturing of high molecular weight polyurethane elastomers (PUs) needs at least two groups as reactants: compounds with isocyanate groups (polyisocyanates, -NHCO-O-) and compounds with hydroxyl groups (polyethers, polyester, etc). PUs are very important products related to their high hardness for given modulus, high abrasion and chemical resistance, excellent mechanical and elastic properties [Petrovic and Ferguson, 1991].

Currently, majority of the hydroxyl groups or most called polyols used for making

polyurethane are derived from petrochemical products. Petrochemicals are based on finite resources of which, optimistic calculations assumed an availability of mineral oil for approximately 50 years. Sooner or later new alternative resources should be prepared or explored. Many years ago, price of mineral oil are as low as compared to the bio-based materials. That is why research on the use of renewable resources is not of the public interests. But in the event of oil crisis and unpredictable price, we must pay more attention on finding an alternative from fossil which is finite to renewable bio-based resources. Amongst

advantages of bio-based materials are their biodegradable, non-toxicity, non-carcinogenicity and renewable resources which are very close to green environmental, because almost all of them are coming from agricultural products [Warwel et al., 2001]. Since it was first synthesized in 1853, many studies on the production of polyol from agricultural products were carried out [Lu et al., 2005; Latere Dwan'isa et al, 2004; Silva Araújo et al., 2004; Uyama et al., 2003]. In the present studies, we are more interested in exploring about the potential of using palm oil as raw materials in polyol production since, almost 80% of worldwide production renewable resources are based on plants oils, i.e. soybean oil, palm oil, sunflower oil, olive oil, tung seed oils etc. Despite the versatility of PUs, they also have some limitations notably having lower thermal stability compared to other polymers. In order to solve this problem, we can employ modified clay montmorillonite (MMT) in the formulations for certain applications. For example, by adding minimum amount (<10 wt. %) of MMT in the formulation, the mechanical and thermal properties of the composites could be enhanced significantly [Wang et al., 2002]. great profits for the community given the

RESEARCH METHODS

This chapter details the preparation and characterization of polyol based on palm oil, synthesis of polyurethane based on palm oil, preparation and characterization of organophilic clay and lastly synthesis and characterization of Polyurethane/clay nanocomposites based on palm oil polyol. The properties of polyol were determined using fourier transform infrared spectra (FTIR) and gel permeation chromatography apparatus (GPC). Organophilic clay was analysis using the X-ray diffraction (X-RD) as an effective method for examining the crystal structure of pristine clay and clay nanocomposites. Finally, Polyurethane/clay nanocomposites were monitored by a pre-polymer method and were evaluated by

fourier transform infrared spectra (FTIR) to determine micro-domain structures. The morphology of the nanocomposites was characterized by X-ray diffraction (X-RD) and flame retardant was investigated with thermogravimetric analysis (TGA). The mechanical properties are analyzed by using instron and dynamic mechanical analysis (DMA). Materials used in this study were: *Kunipia F* (supplied by Kunimine Ind. Co. - it is a Na⁺ type montmorillonite, with a cation exchange capacity of 119 meq/100 g), 4,4-diphenylmethane diisocyanate (MDI, Merck), polyol based on palm oil (patent application no. PI20043190, used materials i.e. : palm oil based oleic acid ; glycerol, system ;4-dodecylbenzenesulfonic acid, fluka ;extruded 3A molecular sieve, Aldrich), 1,4-butanediol (1,4-BDO, Fluka), cetyltrimethyl ammonium bromide (CTAB, Fluka), octadodecylamine (ODA, Merck) and dimethylformamide (DMF, 99%, Fisher) as a solvent. Other inorganic and organic materials that were used in this study were obtained from commercially available source, such as : Natrium Chlorid (NaCl, Merck), Ethyl Alcohol (C₂H₅OH, 95%, System) and Dioxane (Mallinckrodt)

The experiments were carried out in a 250 ml three-necked flask fitted with a mechanical stirrer and a cooling system. The operation conditions were as follows: oleic acid, glycerol, dodecylbenzene sulfonic acid (DBSA), and an extruded 3A molecular sieve. After filtration to remove the molecular sieves, the reaction mixture was washed with a solution of NaCl to remove excess glycerol. Polyol based on palm oil was prepared by the reaction of oleic acid and glycerol. Since the two reactants are not miscible, need to added additives to favor contact between them. Surfactant such as CTAB or DBSA will be producing a homogeneous reaction. In this case, DBSA choose as emulsifier in this system. Because DBSA can work in dual action, as emulsifier and as catalyst. In the presence of DBSA, all esters of glycerol are formed. Although the conversion of oleic acid was elevated, little

glycerol monooleate was formed [Eychenne and Mouloungui, 1999].

The polyurethane-terminated prepolymer was prepared by reacting MDI and polyol at a specified NCO/OH equivalent ratio by using the following procedure. Polyol (12 grams) in DMF was placed in a 0.5L glass reaction kettle, which was equipped with a mechanical stirrer, thermometer, heating mantle and a gas inlet and outlet for continuous flow of nitrogen. When the temperature of the isocyanate reached 70°C, MDI (6 grams) was added in several portions to the reactor under constant mixing. The reaction temperature was maintained at 70°C to 80°C and periodic samples were withdrawn to determine the isocyanate content. After the theoretical NCO% value was reached (using FTIR graph), the reaction was stopped by cooling and the prepolymer stored in a sealed glass bottle under nitrogen. In the second step, the prepolymer was heated at 90-100°C and a specified amount of the prepolymer was weighed into a 250 ml plastic cup. The chain extender (1,4 -BDO) (1.08 grams), which was preheated at 100°C, was added to the prepolymer under vigorous mixing. The TPU films were formed by casting the solution in a mold and remove the solvent under pressure at 70°C. The flow diagram for preparation of polyurethane is shown in Figure 1.

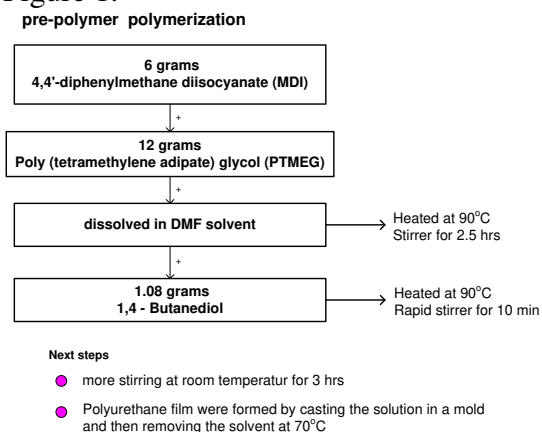


Figure 1 Synthesis of Polyurethane

An amount of 0.05 mol (18.2 grams) of cetyl trimethyl ammonium bromide (CTAB) and 250 mL of distilled water were placed in a

500 ml beaker. These solutions were heated at 80°C for 1 h. Twenty (20) grams of Kunipia-F and 500 ml of distilled water were dispersed in a 1000 ml beaker. The dispersion of *Kunipia-F* was added to the solution of ammonium salt of CTAB, and this mixture was stirred vigorously for 1 h [Yano et al., 1993]. The treated *Kunipia-F* was repeatedly washed by distilled water. The filtrate was titrated with 0.1 N AgNO₃ until there is no chloride or bromide present. The filter cake was then placed for drying in an oven at 60°C. The organophilic *Kunipia-F* was ground and particles of size less than 100 μm were collected by using sieve tray for preparation of nanocomposite. The product was termed CTAB-mont. For the preparation of octadecylamine (ODA-mont), a similar procedure as for the preparation of CTAB-mont was adopted. The flow diagram for preparation of organoclay is shown in Figure 2.2.

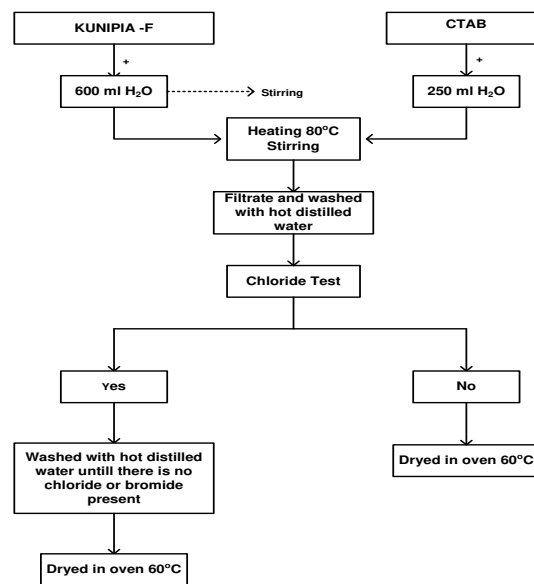


Figure 2 Synthesis of organophilic clays

Polyurethane/clay nanocomposites were prepared by melt blending [Figure 2]. In this study, the amounts of organoclay used in the PU/clay nanocomposites were 1, 3, 5 wt% of polyurethane, respectively. The total volume in each blending was 40 gr. Mixings were carried out using a laboratory internal mixer (Haake Polydrive) at temperature setting of 80°C and a rotor speed of 50 rpm. The

compounds were then compressed using HSINCHU moulded into 1 mm thickness sheets under a pressure of 98×10^5 Pa at 100°C to produce sample sheets [Figure 3.4]. Similar procedures were done for ODA-mont. The physical appearance of clay treated and polyurethane/ clay nanocomposite is inserted in Figure 3



Figure 3 Thermo Haake Polydrive machine

3. RESULTS AND DISCUSSION

This chapter presents the result and discussion of the synthesis of polyurethane based on palm oil polyol, preparation of untreated clay to be clay nanocomposites with difference surfactants i.e. cetyl trimethyl ammonium bromide (CTAB) and Octadecylamines (ODA), synthesis of polyurethane based on palm oil polyol as metric with clay nanocomposites as reinforcement, and determine the efficiency of thermal resistance of polyurethane/ clay nanocomposites with using thermogravimetric analysis (TGA). The result of investigation to determine the micro-domain structures of segmented PU and PU/clay nanocomposites were evaluated by fourier transform infrared spectra (FTIR). The mechanical properties in term of their tensile properties, including the dynamic mechanical properties of pure polyurethane (PU) and PU/clay nanocomposites, were measured. Wide angle x-ray diffraction techniques were utilized to explore the extent of dispersion of clay in filled systems. Furthermore, the molecular weights of materials were determined by Gel Permeation Chromatography apparatus.

Manufacturing polyurethane elastomers (PUEs) needs at least two groups as reactants: compounds with isocyanate groups and compounds hydroxyl groups (polyols). In this study, we are using palm oil as raw materials for production polyol. Oleic acid and glycerol was synthesized by direct esterification in the absence of solvent. Since the two reactants are not miscible, additives was employed to favor contact between them. The employed additives can produce a homogeneous reaction system also and dodecylbenzene sulfonic acid (DBSA) selected as it has both emulsifying and catalytic activity [Eychenne and Mouloungui, 1999].

The preparation of polyol from palm oil based oleic acid and glycerol was monitored by FTIR spectroscopy. Some notable features of the IR spectra include 3384.940 ($\nu\text{O-H}$), 2926.140 ($\nu\text{C-H}$ saturation), 1741.362 ($\nu\text{C=O}$), 1462.932 ($\nu\text{CH=CH}$) and 1174.186 and 1039.892 cm^{-1} ($\nu\text{C-O-C}$) are presented in Figure 3.1 The micro domain structures of the segmented PU were analyzed by FTIR as shown in Figure 4.2. These steps a process synthesis of polyurethane based on palm oil polyol. The collect data start from 0 hour which the peak of isocyanate still in full and finished of synthesis if the peak of isocyanate were disappearances (7 hrs). Following the work by Nunes et al (2000) the degree of phase separation in segmented PU can be estimated. The main regions interested in the study are $-\text{NH}$ absorption peak at 3320 cm^{-1} was due to hydrogen bonded $-\text{NH}$ groups of urethane linkages. The hydrogen bonding was constituted as proton donor and the oxygen in carbonyl of the hard segment and in ether linkages as soft segment. The formation of hydrogen bonding by $-\text{C=O}$ group can be determined by examining the peak position at 1709 cm^{-1} for hydrogen bonded $-\text{C=O}$ and at 1731 cm^{-1} for free $-\text{C=O}$ similar results were reported by Chen (2000).

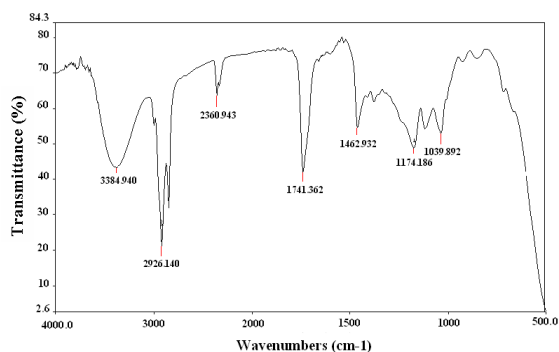


Figure 4 The FTIR spectra of the synthesized polyol based on palm oil

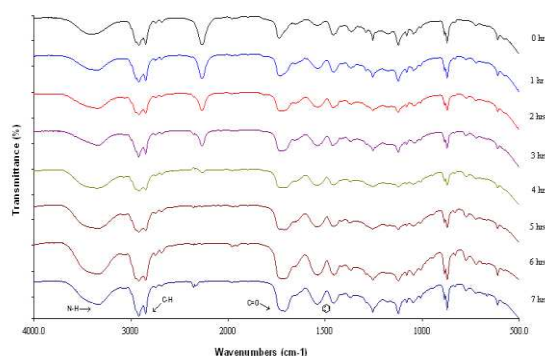


Figure 5 The FTIR spectra of the synthesis polyurethane based on palm oil polyol

The molecular weight (MW) of polyol was obtained by using gel permeation chromatography (GPC). The GPC is also termed size exclusion chromatography (SEC). As suggested by the names, the mechanism of separation in GPC/SEC is based on apparent size differences among the sample components in solutions. There are many techniques for determining the various molecular weight average [Lobo, 2003] such as Number average (M_n), can be obtained by membrane osmometry or end-group analysis, Weight average (M_w) is determined by light scattering, while Z and Z+1 averages (M_z and M_{z+1}) are measured by ultracentrifugation. But GPC is unique in that all these averages can be obtained in a single analysis.

The GPC result of polyol is given in Figure 4 It shows that all the data of various molecular weight average appearance in the below of graphic. The GPC data tabulated possesses the molecular weight averages was about $M_w = 955$ and $M_n = 679$. This

gives dispersity value of 1.4. From the data also show the result of M_z was about 1256. The M_w value that is vital in the synthesis of PU, i.e., the isocyanation process between polyol, MDI and 1,4-BDO. The molecular weight (M_w) of PU based on palm oil was about 3266 [Figure 4.4]. M_n of the products has become 1425 and M_z become 10090. The corresponding dispersity value is 2.29. That is, there is an overall increase in the molecular weight of the sample synthesized. The increase molecular weight value indicating that product is high polymers.

The value in determining the different molecular-weight averages is related to the influence the various molecular-weight fractions have on properties and behavior (Gopakumar and Gopinathan, 2006). For example, additional high-molecular polymer chains may change the flexibility of the polymer to a much greater extent than the same number of low-molecular chains in the material. Raising the molecular weight to higher power in the calculation of M_z than in the calculation of M_n reflects the greater influence of these longer chains. M_z is related to elongation and flexibility, while M_n is related to brittleness and flow properties. Meanwhile M_w is related to characteristics such as tensile strength and impact resistance (Lobo, 2003).

The structure of the segmented polyurethane molecule can be classified into two phases: soft segment and hard segment. Soft segment is obtained by reacting polyol and hard segment is coming from isocyanate. Hard segment associate into rigidity and hydrogen bonding, meanwhile soft segment most conjugated with flexibility (Petrovic and Ferguson, 1991). In the case of synthesis of polyurethane elastomers, the structure segmented polyurethane is important parameters for control of physical properties. GPC is most measurements to determinant the segmented of polyurethane by calculated of molecular weight of the hard segment concentration (HSC) and calculated soft segment concentration (SSC).

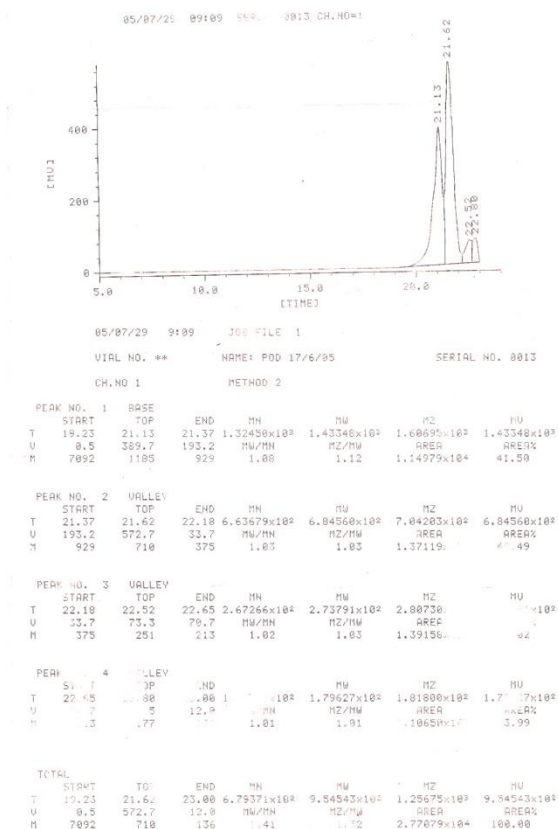


Figure 6 The GPC profiles of the polyol based on palm oil

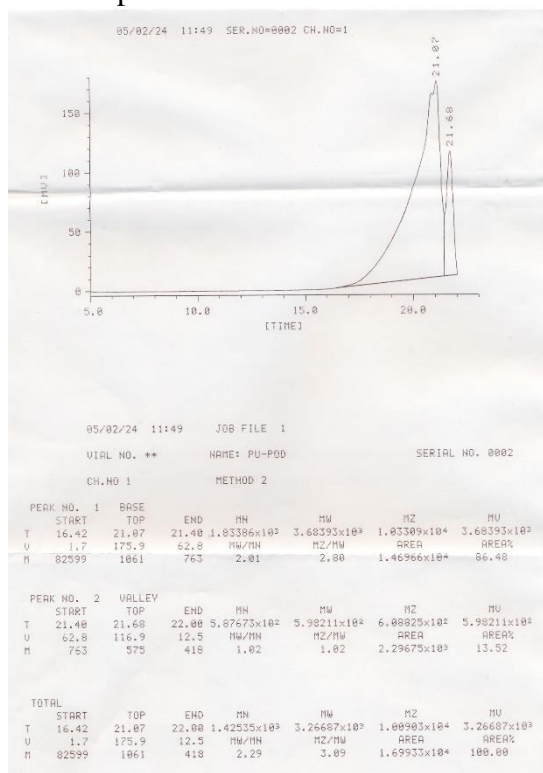


Figure 7 The GPC profiles of the synthesis polyurethane based on palm oil polyol

The flexible (soft) segments in polyurethane elastomers greatly influence the elastic nature of the material and significantly contribute to its low temperature properties and extensibility. Therefore the parameter of soft segment is highly important. Furthermore crystallinity, if any, the melting point, and the possible ability to crystallize with strains, will also certainly influence the ultimate mechanical properties [Jia et al, 2007]

The hard segments in polyurethanes typically consist of an isocyanate and chain-extender glycol or amine components. Structure of the diisocyanate can have a critical influence on the properties of thermoplastic polyurethanes, such as highest levels of modulus, tear, and tensile. The diisocyanate structure apparently influences the ability of the hard segments to pack more regularly and consequently to have higher intermolecular hydrogen bond interaction and a stronger physical network [Chun et al, 2006].

PUs possess good mechanical properties such as high abrasion resistance, tear strength, flexibility and elasticity. However, they also have some limitations by having lower thermal stability compared to other polymers. In order to solve this problem, we can employ modified clay montmorillonite (MMT) in the formulations for certain applications, because by adding minimum amount of MMT (<10 wt. %) in the formulation, the mechanical and thermal properties of the composites could be enhanced significantly [Chen et al., 2001].

Natural montmorillonite has a layered structure made up of disc shaped silicate layers with dimensions of approximately 100 nm in diameters, and 1 nm in thickness. Montmorillonite based clay is hydrophilic and lacks affinity with hydrophobic organic polymers, ion exchange reactions of montmorillonite with various organic cations such as alkylammonium cations rendered the originally hydrophilic silicate surfaces hydrophobic.

If montmorillonite containing sodium ions between its layers is dispersed in water, it

turns into a state in which the silicate layers swell uniformly. If the ammonium salt of alkylamine is added to this aqueous mixture, then the alkylammonium ions are exchanged with the sodium ions. As a result of this reaction, clay forms in which the alkylammonium ions are intercalated between the layers. Because the silicate layers in the clay are negatively charged, they bond with the alkylammonium ions through ionic bonding if an ammonium salt is injected. If the length and type of the alkyl chain are changed, the hydrophilic and hydrophobic characteristics and other characteristics of this organophilic clay can be adjusted such that surface modification of the clay becomes possible. Furthermore the replacement of inorganic exchange cations by organic sodium ions can cause the clay galleries.

The WAXD was used to examine the extent of dispersion of clay in the filled samples. It was also used to measure the silicate layers distribution of the modified clays in the polymer matrix. The montmorillonite (Kunipia-F or termed pure-mont) that was modified with cetyltrimethyl ammonium bromide (CTAB) and octadecylamine (ODA) are termed CTAB-mont and ODA-mont. In Figure 4.5, the *d*-spacing in CTAB-mont and ODA-mont are 1.571 nm and 1.798 nm, respectively, being larger than that of the pure-mont, 1.142 nm. These indicate that both CTAB and ODA were successfully intercalated into the silicate layer.

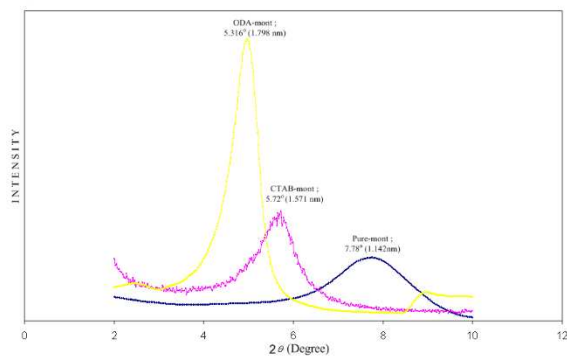


Figure 8 The WAXD pattern of pure-PU

Na⁺ type montmorillonite is composed of sodium ions and negatively charged

montmorillonite. It disperses homogeneously in water, but it does not blend direct in polymer because montmorillonite is too hydrophilic. The hydrophilicity of montmorillonite should be reduced to allow blend in polymer. As montmorillonite has an excess negative charge, it can be combined with organic cations to yield organophilic montmorillonite with organic cations. The scheme is shown in Figure 8

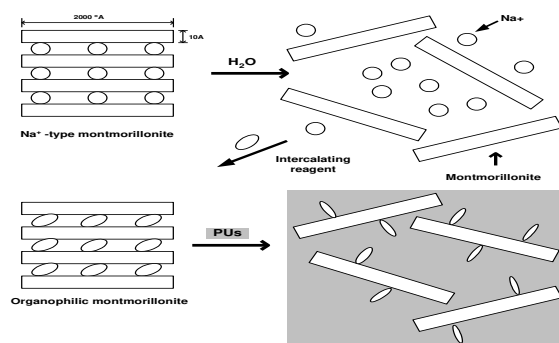


Figure 9 Dispersive behavior of montmorillonite

Figure 8 and 9 present three series WAXD curves of CTAB-mont-PU and ODA-mont-PU that were corresponded to polyurethane clay nanocomposites based on palm oil. In that graphs the appearance of WAXD peaks ($2\theta = 2-10^\circ$) in 1, 3, and 5% CTAB-mont-PU indicated that these organoclay were completely intercalated in polyurethane as matrix. The similar results were obtained for 1, 3, and 5% ODA-mont-PU and as shown in Figure 3.8, the intercalated could also be obtained.

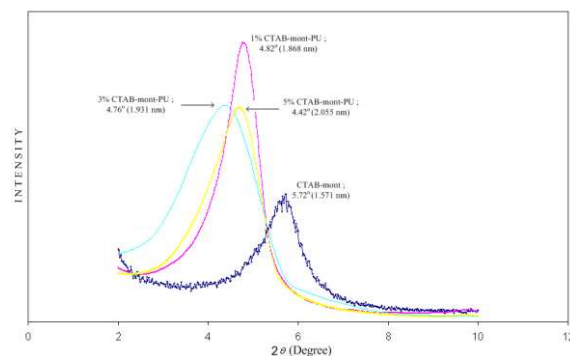


Figure 10 The WAXD pattern of CTAB-mont-PU

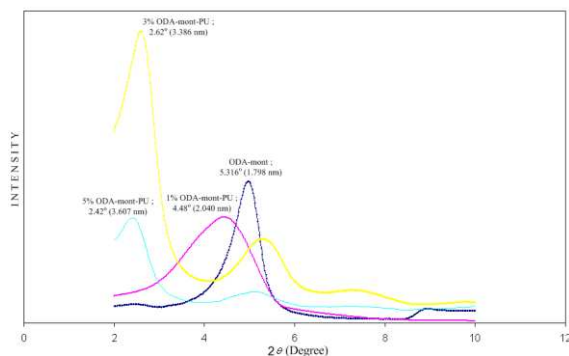


Figure 11 The WAXD pattern of ODA-mont-PU

In the case of 1% CTAB-mont-PU, a very small peak was observed at $2\theta = 4.82^\circ$ (d -spacing = 1.868). With the increasing the clay content, the peak becomes stronger and exhibits a sharp increased peak toward the d -spacing 2.055 nm for 5% CTAB-mont-PU. From the calculation, it was clearly shown that the interlayer spacing of ODA-mont-PU is higher than CTAB-mont-PU. The different swollen spacing in these two organoclays are attributed to the respective size of the swelling agent, with the size of octadecylamine being larger than of cetyltrimethyl ammonium bromide [Chen et al., 2000]. Table 3.1 summaries the d -spacing and 2θ (degree) for CTAB-mont-PU and ODA-mont-PU.

Table 3.1 :Summary of the d -spacing (nm) and 2θ (degree) for Pure Kunipia, CTAB-mont, ODA-mont, CATB-mont-PU and ODA-mont-PU

	2θ (degree)	d -spacing (nm)
Pure Kunipia	7.78	1.142
CTAB-mont	5.72	1.571
ODA-mont	5.31	1.798
1% CTAB-mont-PU	4.82	1.868
3% CTAB-mont-PU	4.76	1.931
5% CTAB-mont-PU	4.42	2.055
1% ODA-mont-PU	4.48	2.040
3% ODA-mont-PU	2.62	3.386
5% ODA-mont-PU	2.42	3.607

The microdomain and the hydrogen bonding of segmented PU and the PU/clay were analyzed FTIR. It was found that the positions of peaks for distinctive functional groups in the IR spectra of the pure PU and PU/clay nanocomposites are identical, which means that the chemical structures of polyurethane had not been affected by the presence of organoclay, which implied that

either the organic modified silicate layers did not react with the PU molecules or reactions between organic modified silicate layers, thus indicating that PU did not cause any detectable change by FTIR.

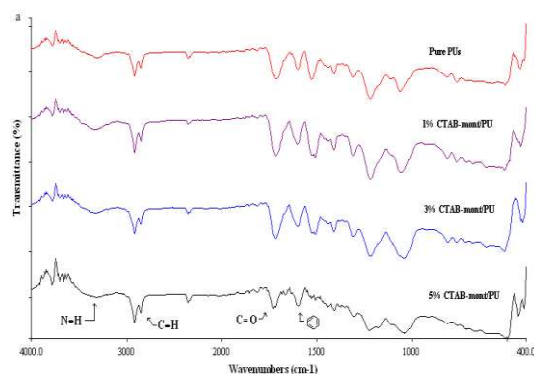


Figure 12 The FTIR spectra of pure PU and 1,3,5% CTAB-mont-PU

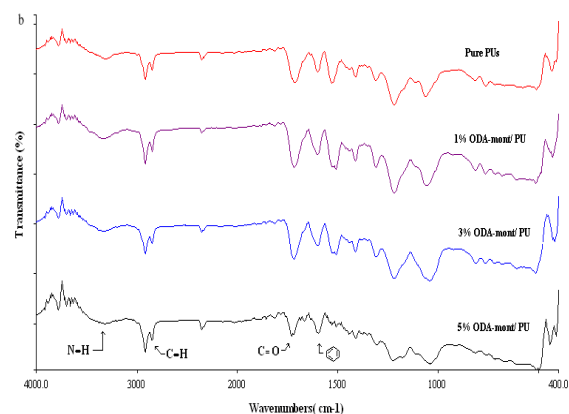


Figure 13 The FTIR spectra of pure PU and 1,3,5% ODA-mont-PU

Therefore, the effect of the intercalated silicate layers on the degree of phase separation in polyurethane can be determined solely from the extent of hydrogen bonding in the hard segments and the degree of hydrogen bonding in these polyurethane nanocomposites can be obtained from their IR spectra also.

From the investigation by Pattanayak and Jana (2005) that has been studied the nature and behavior of hydrogen bonding in segmented polyether and polyester urethane elastomers, it has been concluded that at 3320 cm^{-1} peak and 3480 cm^{-1} peak in the IR spectra of pure PU are due to hydrogen bonded -NH groups and free -NH groups

respectively. The hydrogen bonding was constituted by the –NH groups being as proton donor and oxygen in carbonyls of the hard segment and in ethers of the soft segment as proton acceptors. The formation of hydrogen bonding can be determined by examining the peak position of free urethane carbonyl and hydrogen bonded carbonyl. The peak at 1733 cm⁻¹ is assigned to free the urethane carbonyl, while the peak at 1703 cm⁻¹ is due to hydrogen bonded carbonyl [Tien and Wei, 2001 ; Dai et al., 2004]. The standard assignment of vibration modes the absorption band of these groups are listed in Table 3.2.

Table 3.2 : Assignments of the Absorption Bands in FT-IR Spectra of Polyurethane (modified from Pattanayak and Jana (2005) ; Tien and Wei, 2001 ; Dai et al., 2004)

Freq. (cm ⁻¹)	assignment	domain origin
3480	v(NH), free	hard segment
3320	v(NH), hydrogen-bonded	hard segment
2935	v(CH ₂), free	soft segment
1733	v(C=O), free urethane carbonyl	hard segment
1703	v(C=O), Hydrogen bonded	hard segment

The degree of the carbonyl groups participating in hydrogen bonding can be described by the carbonyl hydrogen bonding index, R, as given in Eq. (4.1).

$$R = \frac{C_{\text{bonded}} \epsilon_{\text{bonded}}}{C_{\text{free}} \epsilon_{\text{free}}} = \frac{A_{1703}}{A_{1733}} \dots\dots\dots (4.1)$$

where A is the intensity of the characteristic absorbance, C is the concentration and ε_{bonded} and ε_{free} are the extinction coefficients of the bonded and the free carbonyl groups, respectively. The value of ε_{bonded} / ε_{free} was between 1.0 and 1.2 [Jia et al. 2007 ; Rekondo et al. 2006]. In this study, the value of ε_{bonded} / ε_{free} is taken as 1.0, and the carbonyl hydrogen bonding index is directly equal to the ratio of the normalized absorbance intensity in 1703 cm⁻¹ to that in 1733⁻¹. The degree of hard segment linking hard segment (degree of phase separation, DPS) and the degree of hard segment linking soft segment or silicate layers (degree of phase mixing, DPM) can be obtained readily

by using Eqs. (4.2) and (4.3), respectively [Chen et al., 2000].

$$DPS = \frac{C_{\text{bonded}}}{C_{\text{bonded}} + C_{\text{free}}} = \frac{R}{R+1} \dots\dots\dots (4.2)$$

$$DPM = 1 - DPS \dots\dots\dots (4.3)$$

Table 4.3 : Absorption of carbonyl and degree of phase separation

	$\frac{A_{1702}}{A_{1731}}$	DPS (%)	DPM (%)
Pure PU	0.9288	48.10	51.90
1% CTAB-mont-PU	0.9625	49.04	50.95
3% CTAB-mont-PU	0.9287	48.15	51.85
5% CTAB-mont-PU	0.9623	49.03	50.97
1% ODA-mont-PU	0.9637	49.07	50.93
3% ODA-mont-PU	0.9612	49.01	50.99
5% ODA-mont-PU	0.9617	49.02	50.98

Based on these calculations, the DPS and DPM values of organoclay/PU nanocomposites are given in Table 4.3. As indicated in Table 4.3, the phase separation ratio in pure PU is about 52%. There was almost no change in DPS and DPM of all CTAB-mont/PU and ODA-mont/PU nanocomposites, indicating no dependence on the amount of added organoclay. This can be explained by a uniform dispersion of intercalated silicate layers of organoclay in the nanometer scale in PU matrix, which cannot be matched by the classical composite materials. Similar phenomena were also observed by Pattanayak and Jana (2005 a); Gorrasi et.al. (2005).

The MW of pure PU and PU/ clay nanocomposites are given in Table 4.4. Pure PU had MW of 3915.19, 1% CTAB-mont-PU had MW of 4160.33, 3% CTAB-mont-PU had MW of 4360.29 and 5% CTAB-mont-PU had MW of 4417.25 while 1% ODA-mont-PU had MW of 4245.12, 3% ODA-mont-PU had MW of 4429.45 and 5% ODA-mont-PU had MW of 4610.11. In each case, corresponding to the fact that the segmented PU structures were affected by the presence of organoclay as identified by their FTIR spectra, the molecular weight of pure PU and PU/ clay nanocomposites in general were not strongly affected by the addition of organoclay, this result is similar with the research by T.-K. Chen et al (1999).

Table 3.4: The number-average molecular weight and mechanical properties of Pure PU and PU/clay nanocomposites

	MW	Tensile strength (MPa)	Elongation at break (%)
Pure PU	3266.19	14.983	253.4
1% CTAB-mont-PU	3960.33	21.766	270.7
3% CTAB-mont-PU	3809.29	28.342	415.3
5% CTAB-mont-PU	3917.25	32.178	431.1
1% ODA-mont-PU	3745.12	30.491	490.0
3% ODA-mont-PU	3929.45	39.257	677.9
5% ODA-mont-PU	3810.11	40.100	700.5

The mechanical properties of PU and PU/clay nanocomposites are given in Table 3.4, Figures 14 and 15. The modified organoclay had a remarkably beneficial effect on the strength and elongation at break of the nanocomposites, which both increased with increasing clay content, the ODA treated varieties having the highest values. The fact that the elongation at break of the nanocomposites increased with the organoclay content suggests that elongation was related to the interaction between the pure PU and the treated clays [Rihayat et al, 2007]

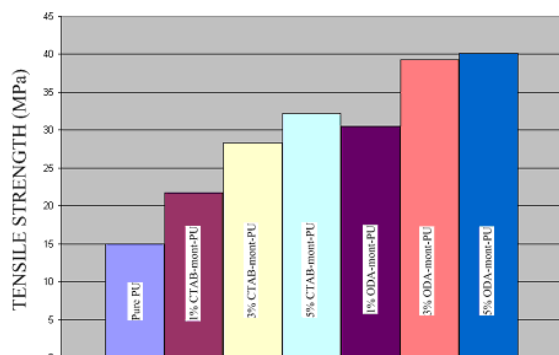


Figure 14. Tensile strength of pure PU and PU/clay nanocomposites

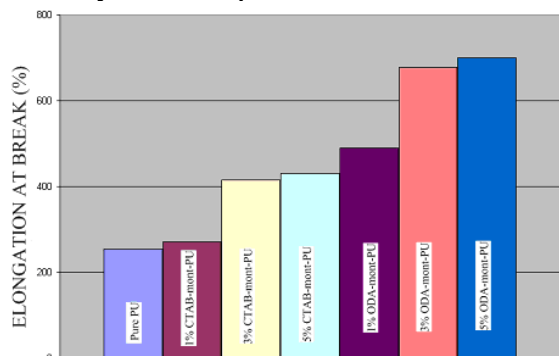


Figure 15 Elongation at break of pure PU and PU/clay nanocomposites

As shown in Table 3.4, and Figure 3.11, the ultimate strength was increased dramatically with the increasing of the organoclay content and has reached maximum values at 5 wt% organoclay content with the increase of the tensile strength of more than 214.76% and 267.63 % by the addition of only 5% of the montmorillonite CTAB-mont and ODA-mont respectively. Furthermore Table 4.4 and Figure 15 also illustrate that the elongation at break of the nanocomposites were increased with the addition of organoclay content, which means it was related to the interaction between the pure PU and treated clays [Xiong et al, 2004]. The graphics in Figures 14 and 15 also explains that the tensile strength and elongation at break value of the polyurethane containing octadodecylamine (ODA-mont) was usually higher than that of cetyltrimethyl ammonium bromide (CTAB-mont), it was indicated a strong effect of ODA-mont on polyurethane. Most applications of elastomers would be impossible without the reinforcement of certain fillers, such as carbon black, clay, etc. Reinforcement is usually associated with improvement in modulus, hardness, and tensile and tear strength of vulcanized materials.

The modulus reinforcement of Pus-clay nanocomposites was examined using Guth, Halping-Tsai and the modified Halping-Tsai equations, which are universally used for composites reinforced by fiber-like or rod-like filler. Experiments have been performed to measure Young's modulus of the nanocomposites in the direction of the aligned platelets for Pus-clay nanocomposites of different clay concentration. The results are shown in Table 3.5 : Measured tensile modulus E for Pus-clay nanocomposites

	Wt% clay	Tensile modulus (MPa)
Pure PU	0	118.694
1% CTAB-mont-PU	1	127.252
3% CTAB-mont-PU	3	130.688
5% CTAB-mont-PU	5	140.575
1% ODA-mont-PU	1	130.798
3% ODA-mont-PU	3	132.781
5% ODA-mont-PU	5	144.550

Figure 16 compares experimental modulus data of 1,3, 5 wt% of CTAB-mont-PU and ODA-mont-PU, respectively, with the model predictions using the parameter values in Table 4.3. The results show that the predictions by Guth equation agree very well with the experimental data; whereas the Halpin–Tsai equation can only be applied to predict the modulus of rubber–clay nanocomposites in the range of low clay volume fractions, for example, less than 1 wt%.

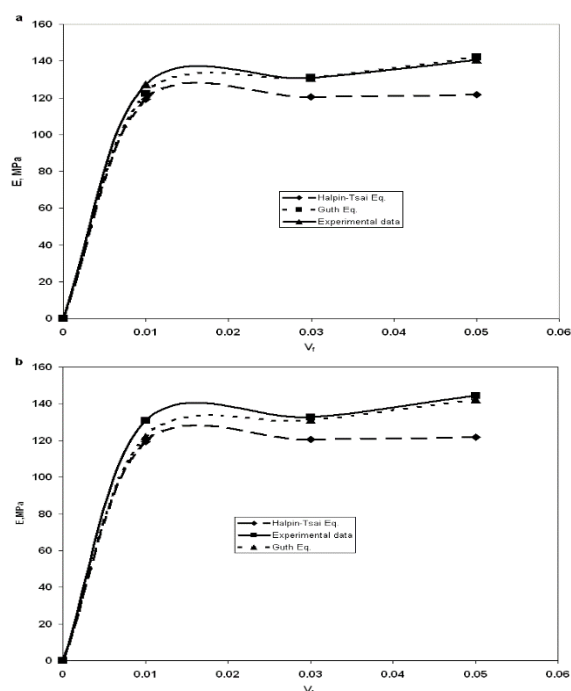


Figure 16 Experimentally measured modulus and theoretical predictions by two different models: Guth and Halpin-Tsai equations for (a) CTAB-mont-PU and (b) ODA-mont-PU.

According to the Halpin-Tsai theory of filler reinforcement, volume fraction and aspect ratio are key parameters governing the mechanical properties of composites. In the formation of nanocomposites, clay platelets initially stacked together to form clay particles are intercalated with polymer, exfoliated and dispersed in the polymer matrix. A single platelet layer is sheet like, having a thickness of only about 1 nm and lateral dimensions that are typically on the order of 500-2000 nm [Ray and Okamoto,

2003]. The theoretical prediction for modulus behavior investigated above suggested that the resulting aspect ratio of 1000, with 3 wt% clay for example, is a contributing reinforcing factor. Such high aspect ratio silicate platelets could be present in exfoliated systems where individual platelets separate from the clay stack and are dispersed in the polyurethane matrix. In order to see if this is the case, x-ray diffraction (XRD) was conducted to explore the microstructure of PUs-montmorillonite composites.

Table 3.5 showed the summarized of tensile modulus. The enhancement of tensile modulus is directly attributed to the reinforcement provided by the dispersed silicate layers and Young's modulus can also be affected by the interfacial interaction between silicate layers and polyurethane matrix. Therefore, Young's modulus increased with increasing the clay content and the dispersibility of organoclay. The largest increase in Young's modulus (144.550 MPa) was shown at 5% ODA-mont-PU. As mentioned above, there are two strong interactions between polyurethane matrix and layered silicates such as the hydrogen bonding and the chemical bonding, so the tensile strength and elongation at break increased by introducing organoclay. Because the interfacial area between organoclay and polyurethane matrix became larger and the interaction between organoclay and polyurethane matrix became also stronger, the tensile modulus of ODA-mont-PU was significantly higher than that of CTAB-mont-PU and pure polyurethane.

The dynamic mechanical analysis (DMA) was performed to examine the effect of the clays on the structure, concentration and organization of the hard-segments, and their interaction with the soft segments, have a dominant influence on the physical and mechanical properties of the urethane polymer [Abdalla et al, 2002]. The loss factors ($\tan \delta$) value of pure PU and PU/clay nanocomposites are presented in Figure 3.14

and 3.15. Treated clay seems to be more efficient for increasing the glass transition temperature (T_g). According to Choi et al (2004) and Agag et al (2001), it was confirmed that the T_g increase with the increased of the clay content resulting from the confinement effect of clay to polyurethane molecules and the strong interactions of hydrogen bonding in between the urethane groups of polyurethane molecules and oxygen atoms on the surface of organoclay.

In Figure 3.14, the T_g of CTAB-mont-PU were -11.776°C , -8.113°C and -6.764°C for clay content of 1%, 3% and 5%, respectively. Those values are higher than pure PU which was: -12.200°C . But in fig 3.15 the T_g of ODA-mont-PU is higher than the T_g of CTAB-mont-PU with the results (for the ODA-mont-PU sample) are -11.114°C , -6.5°C and -5°C at the similar clay contents respectively.

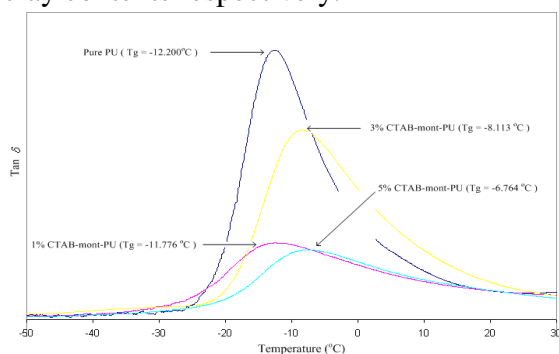


Figure 3.14. DMA curves for $\tan \delta$ of pure PU and CTAB-mont-PU 1, 3, 5 wt%

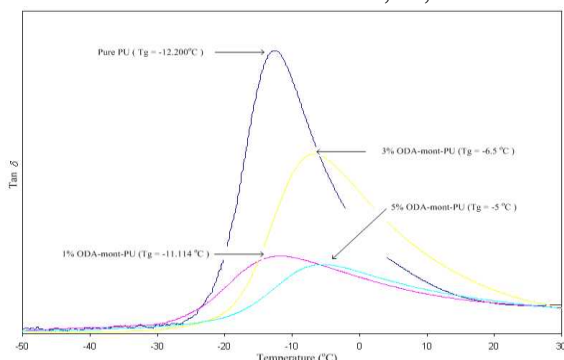


Figure 3.15. DMA curves for $\tan \delta$ of pure PU and ODA-mont-PU 1,3,5 wt%

The thermal properties were determined using Thermogravimetric analysis (TGA). During a ramped heating under nitrogen, such as in a TGA experiment, the

degradation process usually passes through three stages. In the first and second stage, the urethane bonds decompose to form alcohols and isocyanates. Complete volatilisation of resulting chain fragments is prevented by dimerisation of isocyanate to carbodiimides, which react with the alcohol groups to give relatively stable substituted ureas (second step) that decompose in the third stage. Trimerisation of isocyanates may also occur under certain conditions to yield thermally stable isocyanurate rings. The final step is the high temperature degradation of these stabilized structures to yield volatile products and a small quantity of carbonaceous char. The TGA analysis of pure PU, CTAB-mont 1, 3, 5 wt% and ODA-mont-PU 1, 3, 5 wt%, respectively, are shown in Figure 4.16 and 4.17. With regard to pure PU, the degradation at 200-400 °C is attributed to depolycondensation reaction. Then at higher temperature, the material degrades slowly, and it degrades completely at about 700°C. The results show that thermal resistances are enhanced in the presence of clay compared to pure PU. This indicates an improvement in thermal stability of PU because the organic material can prevent the heat from expanding quickly and limit the further degradation. Onset degradation of pure PU is at 200°C, and is lower than of the CTAB-mont-PU and ODA-mont-PU takes place at about 318°C and 330°C. It means the thermal resistance of nanocomposites improved above 62% compared pure polymer. But in overall thermal resistance of ODA-mont-PU nanocomposites was much higher than that of pure PU and CTAB-mont-PU.

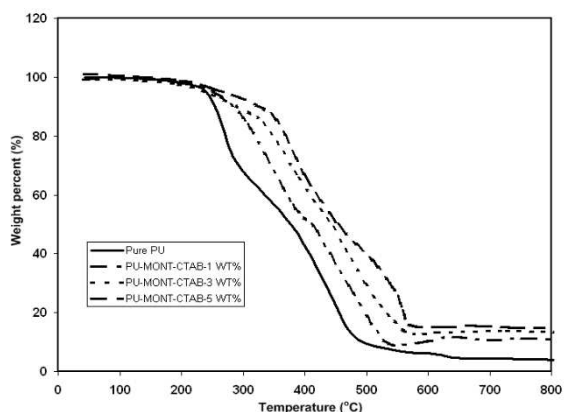


Figure 4.16. The TGA curves of pure PU and PU/clay nanocomposites CTAB-mont-PU 1, 3, 5 wt%

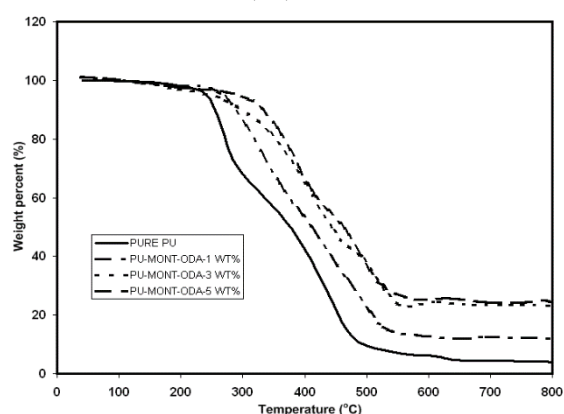


Figure 4.17. The TGA curves of pure PU and PU/clay nanocomposites ODA-mont-PU 1,3,5 wt%

From the graphic analysis showed of CTAB-mont-PU and ODA-mont-PU in the temperature range from 100 to 275°C, the PU/clay nanocomposites contain swelling agent (CTAB and ODA) degrades slightly faster than pure PU, especially in 1 and 3 wt%. This is because the amount of CTAB and ODA used increased with the amount of organoclay in PU. These small organic molecules tend to degrade before the PU polymer, causing a slight weight loss in the nanocomposites. After a complete decomposition of the swelling agent, the PU/clay nanocomposite displayed higher thermal resistance than that of PU in the temperature range above 400°C because of the presence of clay. This indicating inorganic material can prevent the heat to expand quickly and limit the further degradation.

Only single heating rate, pseudo first order method has been applied in this study. Figures 4.18-4.24 show the plot of $\ln[-(dw/dt)/w]$ against $-1/T$ for the pure PU and PU/ clay nanocomposites 1, 3, 5 wt%, respectively, on the basis equation (3.10) from section 3.7.8 (Chapter III), if the reaction is first order, it should be expected that the data calculated from TGA thermograms base on equation (3.17) could be fitted by a straight line of the slope equal to activation energy, E , and intercept equal to $\ln A$, where A is pre-exponential or frequency factor. The values of E and A calculated following the approach described above are summarized in Table 4.6. The E value of the materials can be used to determine whether the initial degradation step [Gu and Liang, 2003]. As can be seen from Table 4.6 the clay had a great effect on activation energy of nanocomposites and pristine polyurethane, especially for 5 wt% CTAB-mont PU and 5 wt% ODA-mont PU. Table 3.6:A summary of the kinetics parameters obtained using the simple linear regression method.

	E (J/mol)	$\ln A$ (min ⁻¹)
Pure PU	187.150	7.1333
1% CTAB-mont-PU	1437.657	3.0050
3% CTAB-mont-PU	1563.448	2.4726
5% CTAB-mont-PU	1863.001	1.6555
1% ODA-mont-PU	1528.695	2.6075
3% ODA-mont-PU	1585.230	1.2755
5% ODA-mont-PU	1960.026	1.0434

From the data clearly indicate that the long chain molecular motion in the PU-clay nanocomposites encounters a markedly larger energy barrier than it does in pure PU. That is at the same temperature the nanocomposite should have lower molecular mobility than the pure polymer. Because the molecular mobility is the major factor that contributes to the transport of reactive species (e.g., oxygen and or/or radicals) within the polymer, the nanocomposite is likely to have lower reactivity and, therefore, greater chemical and thermal stability than pure PU [Vyazovkin et al, 2004]

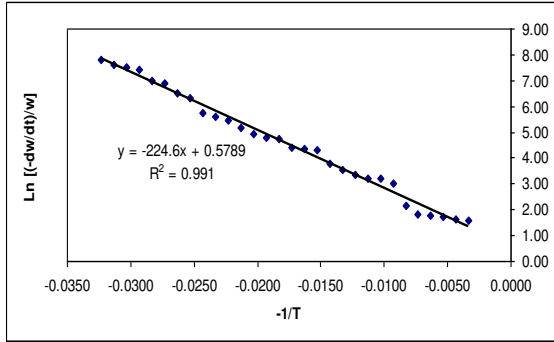


Figure 3.18: First order kinetic plot for pure Polyurethane

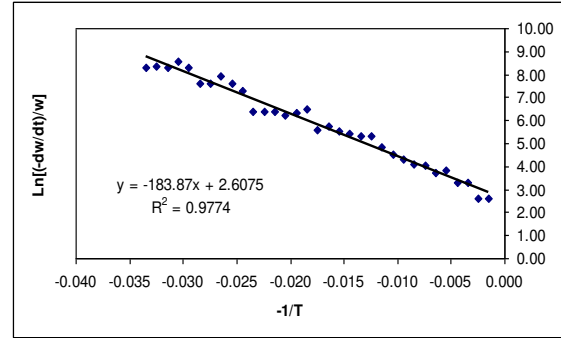


Figure 3.22: First order kinetic plot for PU/Clay nanocomposites ODA 1 wt%

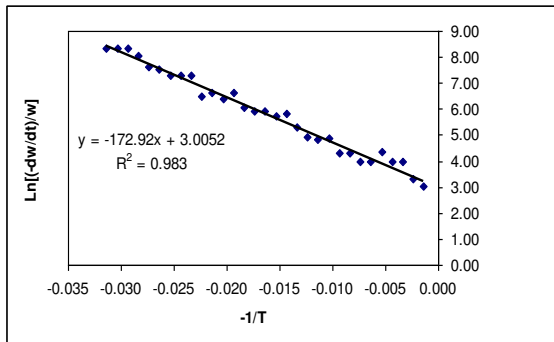


Figure 3.19: First order kinetic plot for PU/Clay nanocomposites CTAB 1 wt%

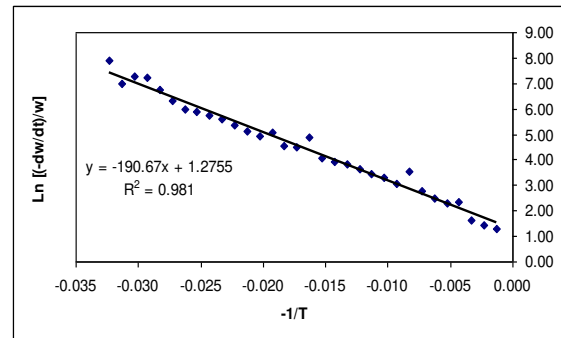


Figure 3.23: First order kinetic plot for PU/Clay nanocomposites ODA 3 wt%

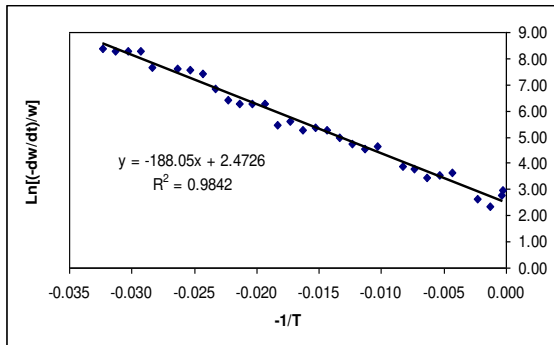


Figure 3.20: First order kinetic plot for PU/Clay nanocomposites CTAB 3 wt%

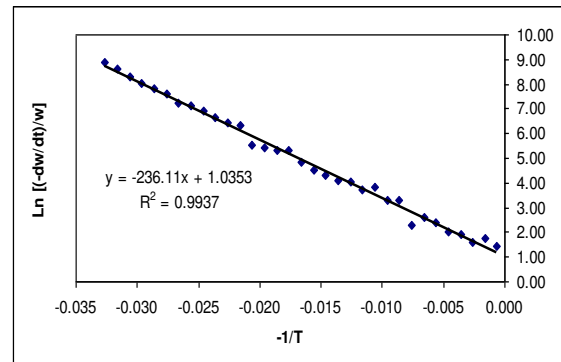


Figure 3.24: First order kinetic plot for PU/Clay nanocomposites ODA 5 wt%

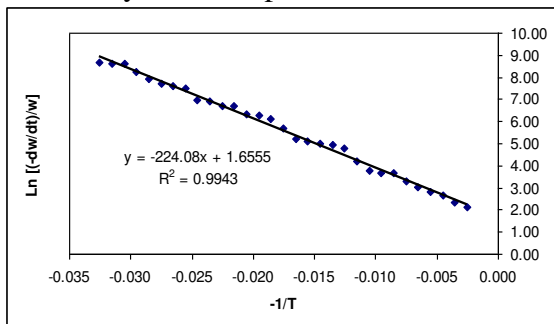


Figure 3.21: First order kinetic plot for PU/Clay nanocomposites CTAB 5 wt%

In figures 3.25 and 3.26, morphological observations on the fractured surfaces of the PU and PU/clay nanocomposites samples are shown. The filler employed as reinforcements for polymers and resins are invariably coated with sizing resin whose role to protect them during handling and impregnation. Furthermore the filler surface is treated to provide chemical interactions with the polymer employed as the matrix. The net result of SEM is that the nature of

differing interactions such as the physical mixing of the matrix and sizing resins and the nature of chemisorptions at the filler surface gives rise to a interphase region as opposed to a distinct interface between nanoclay and polymer matrix [Lam et al, 2005].

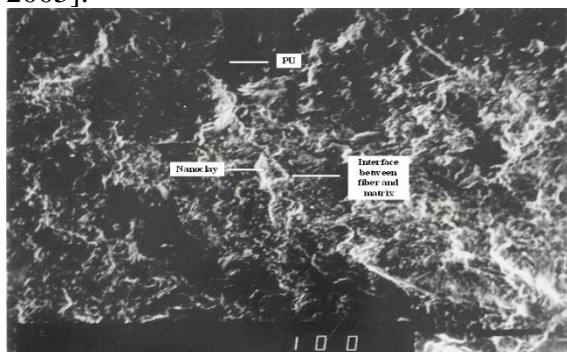


Figure 3.25. SEM micrographs of interfacial adhesion between nanoclay and matrix PU

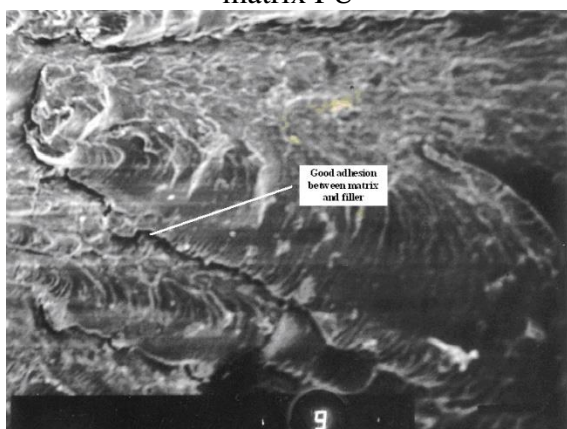


Figure 3.26. SEM micrographs of a good dispersion between nanoclay and ODA-Mont-PU 3 wt%

Jayaraman (2003) studied the fibers and matrix must cooperate for a composite to be an effective load bearing. This corporation between the fillers and matrix will not exist without the presence of the interface. The interface acts as a binder and transfer load between the matrix and the reinforcing fillers. Further, because each filler forms an individual interface with the matrix, the interfacial area is very large. The interface, therefore, plays a key role in controlling the mechanical properties of a composite. The role of the matrix in the fiber-reinforced composite is to transfer the load to the stiff fiber through shear stress at the interface. This process required a good bond between

the polymeric matrix and the filler [Wambua et al, 2003]. The interface between fiber and matrix is shown below in Figure 3.25

In Figure 3.26 show ODA-Mont-PU 3 wt% has a good dispersion between matrix and fiber. Duquesne et al. (2003) studied the better dispersion between nanoclay and polymer matrix. The bright spots on the backscattered images correspond to clay aggregates. Figure 3.26 presents the microstructure of a nanocomposite with 3 wt% of organoclay. The clay particles are finely dispersed in the material. Moreover, the finest dispersion can probably not be detected by SEM. Apparently, the clay particles are more finely dispersed in the nanocomposite as compared with in the conventional composite. This difference must be due to the treatment of the clay. The alkylammonium ions render the clay organophilic and allow a better dispersion of the clay in an organic medium. Small particle aggregates are observable at relatively low magnification.

Figure 3.27-3.32 shows the transmission electron micrograph of sections of the PU/Clay nanocomposites. The dark lines are intersections of silicates layers, and the other region is PU matrix. It can be seen that silicate layers have reached nanometer scale and effectively intercalated or exfoliated in the PU matrix. Observations of the micrograph reveal that each dark line often corresponds to several clay layers [Kornmann et al, 2001]. In some cases, this is because the layers are closely stacked together, suggesting the absence of alkylammonium ions in the galleries.

The TEM image of the PU/clay nanocomposites showed that the clay particles were broken into small tactoids and uniformly dispersed in the PU matrix, which resulted from strong interaction between clay and polymer and it is imperative that the surface polarities of the polymer and clays or organoclays be matched [Park et al, 2002] Figures 3.27 and 3.28, TEM photograph of PU/Clay nanocomposites CTAB 1 wt% and ODA 1 wt% show that clay layers are completely intercalated when 1% clay were

added into PU matrix. Figures 3.29 and 3.30, exhibits a well-intercalated and exfoliated structure. At the other image in figures 3.31 and 3.32, show fine and almost uniform distribution of clay particles in the PU matrix where the clay particles exhibit both stacked and flocculated to the sample surface and an intercalated structure has been produced. The presence of exfoliated clay layers at higher concentration probably caused by high shear impact on the mixture. As shear mixing progress, the molten polymer becomes more and more viscous with the dispersion of clay particles. At higher clay content the viscosity will help the delamination of silicate layers and also intercalation of the polymer chains into the silicate layers therefore increase the basal spacing of clay platelets in the PU matrix (Fornes et al., 2001).

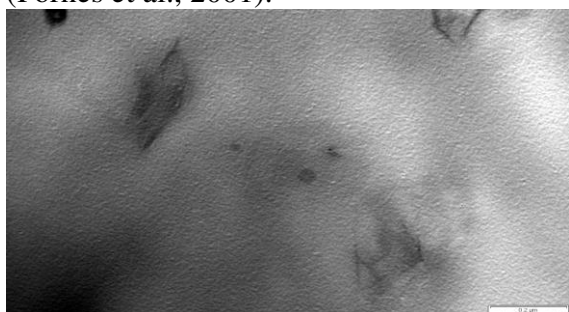


Figure 3.27. TEM photograph of PU/Clay nanocomposites CTAB 1 wt%

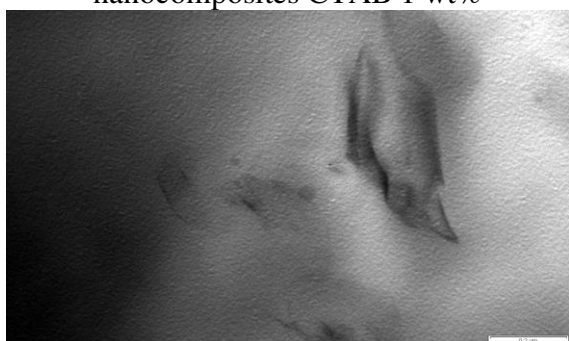


Figure 3.28. TEM photograph of PU/Clay nanocomposites ODA 1 wt%

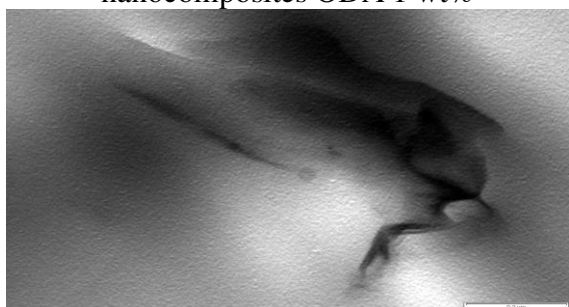


Figure 3.29. TEM photograph of PU/Clay nanocomposites CTAB 3 wt%

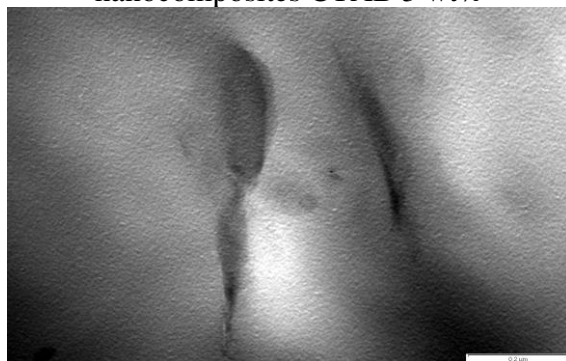


Figure 3.30. TEM photograph of PU/Clay nanocomposites ODA 3 wt%

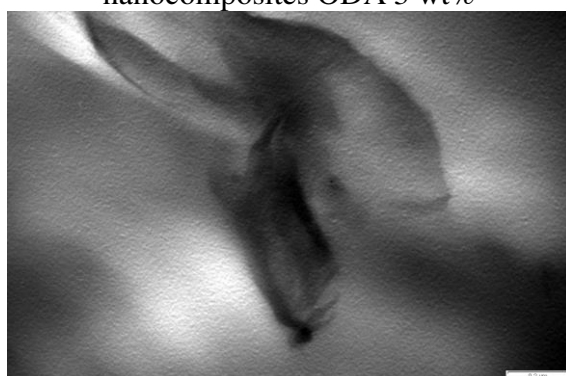


Figure 4.31. TEM photograph of PU/Clay nanocomposites CTAB 5 wt%

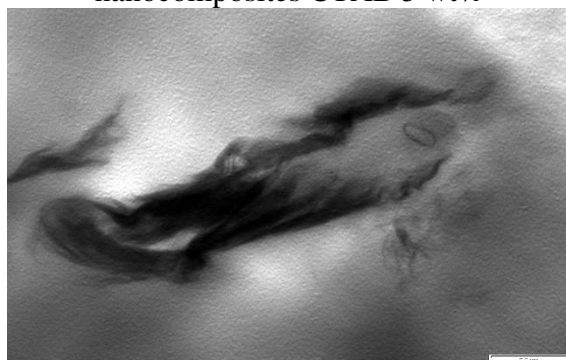


Figure 4.32. TEM photograph of PU/Clay nanocomposites ODA 5 wt%

CONCLUSION

Isocyanate groups (polyisocyanates, -NHCO-O-) and hydroxyl groups (polyethers, polyester, etc.) are required as reactants for the production of high molecular weight polyurethane elastomers (PUs). PUs are very significant goods that have great mechanical and elastic qualities, high hardness for a given modulus, and strong abrasion and chemical resistance. The majority of the hydroxyl groups, also known

as polyols, now utilized to make polyurethane come from petrochemical goods. Mineral oil, which is a finite resource whose supply has only been anticipated to last for about 50 years in optimistic projections, is the source of petrochemical products. Other potential sources should be found or investigated sooner or later.

Since about 80% of the world's production of renewable sources is based on plant oils, such as soybean oil, palm oil, sunflower oil, olive oil, and seed oils, among others, the options used in this research work to use palm oil as a raw material in polyol synthesis are quite interesting. Glycerol and palm oil (bought from a local manufacturer) based on oleic acid were combined to create polyols. The polyols could also be utilized as starting materials for the isocyanation of isocyanate compounds to produce polyurethanes.

FTIR spectroscopy was used to track the production of polyol from glycerol and oleic acid derived from palm oil. Gel permeation chromatography (GPC) was used to determine the molecular weight (MW) of polyol, and the result was around 950.

Following Seymour et al.'s research, the segmented PU microdomain structures were examined by FTIR to determine the degree of phase separation. By comparing the peak positions at 1709 cm^{-1} for hydrogen bound $-\text{C}=\text{O}$ and at 1731 cm^{-1} for free $-\text{C}=\text{O}$, it is possible to ascertain the establishment of hydrogen bonding by the $-\text{C}=\text{O}$ group. The molecular weight (MW) of the palm oil-based PU was around 3.266.

Because of ion exchange interactions between montmorillonite and other organic cations, such as alkylammonium cations, the initially hydrophilic silicate surfaces became hydrophobic, making montmorillonite-based clay hydrophilic and lacking affinity for hydrophobic organic polymers. The silicate layer distribution of the modified clays in the polymer matrix was examined using the WAXD, and the degree of clay dispersion in the filled samples was also measured. The terms "CTAB-mont" and "ODA-mont" refer to the montmorillonite (Kunipia-F or "pure-mont") that has

undergone chemical modification using cetyltrimethyl ammonium bromide (CTAB) and octadodecylamine (ODA). As a result, the d-spacing of CTAB-mont and ODA-mont is bigger than that of pure-mont, which is 1.142 nm, at 1.571 nm and 1.798 nm, respectively. These show that the silicate was successfully intercalated with both CTAB and ODA.

The morphology, mechanical and thermal properties that have been investigated in this study were corresponded to the disperse of organoclay in the polyurethane matrix. The treated clays were completely intercalated in polyurethane matrix and the intercalation effects were increased with the increasing of the clay contents. In the appearance of WAXD peaks ($2\theta = 2-10^\circ$) in 1, 3, and 5% CTAB-mont-PU indicated that these organoclay were completely intercalated in polyurethane as matrix. The similar results were obtained for 1, 3, and 5% ODA-mont-PU. The microdomain and the hydrogen bonding of segmented PU and the PU/clay were analyzed FTIR. It was found that the positions of peaks for distinctive functional groups in the IR spectra of the pure PU and PU/clay nanocomposites are identical, which means that the chemical structures of polyurethane had not been affected by the presence of organoclay.

The mechanical properties of PU and PU/clay nanocomposites were studied in this work. It was found that the modified organoclay content had a remarkable effect on the strength of the nanocomposites. The tensile strength and elongation at break increased more than 200%, which could be assumed as a result of the strong interaction between treated clay and polyurethane as nanocomposites. The dynamic mechanical analysis was employed to examine the effect of clay contents on the thermomechanical properties and microstructure of the material and it was found that, the glass transition (T_g) was increased with the increasing of the clay contents, which was assumed as a result of the confinement effects of clay to polyurethane molecules and the strong

interactions such as hydrogen bonding between the urethane groups of polyurethane molecules and oxygen atoms on the surface of organoclays.

The thermal properties were determined using TGA. The TGA analysis of pure PU, CTAB-mont 1, 3, 5 wt% and ODA-mont-PU 1, 3, 5 wt%, respectively. With regard to pure PU, the degradation at 200-400 °C is attributed to depolycondensation reaction. Then at higher temperature, the material degrades slowly, and it degrades completely at about 700°C. The results show that thermal resistances are enhanced in the presence of clay compared to pure PU. This indicates an improvement in thermal stability of PU because the organic material can prevent the heat from expanding quickly and limit the further degradation. Onset degradation of pure PU is at 200°C, and is lower than of the CTAB-mont-PU and ODA-mont-PU takes place at about 318°C and 330°C. It means the thermal resistance of nanocomposites improved above 62% compared pure polymer.

Morphological observations on the fractured surfaces of the PU and PU/clay nanocomposites samples were determined by SEM and TEM. The result show clay particles are finely dispersed in the material.

REFERENCES

- Abdalla, M.O., Dean, D. and Campbell, S. **2002**. Viscoelastic and mechanical properties of thermoset PMR-type polyimide-clay nanocomposites. *Polymer* 43: 5887
- Ahmad, S., Leong, Y.C., Mohamed, I. and Ong, E.L. **1987**. Proc.1987. Int.Oil Palm/Palm oil Conf.(Conf. II: Technology), Kuala Lumpur, Malaysia, organized by PORIM/ISP.
- Ahmadi, S.J., Huang, Y.D. and Li, W. **2004**. Review synthetic routes, properties and future applications of polymer-layered silicate nanocomposite. *Journal of materials science* 39: 1919-1925
- Agag, T., Koga, T. and Takeichi, T. **2001**. Studies on thermal and mechanical properties of polyimide-clay nanocomposites. *Polymer* 42: 3399-3408.
- Alexandre, M and Dubois, P. **2000**. Polymer-layered silicate nanocomposites: preparation, properties and uses of a new class of materials. *Materials Science and Engineering: R: Reports* 28: 1-63
- Alexandrovich, P.S., Karasz, F.E. and Macknight, W.J. **1980**. Dielectric study of polymer compatibility: Blends of polystyrene/poly-2-chlorostyrene. *J. Macromolec. Sci. Phys.*, B17: 501.
- Anseth, K.S, Bowman, C.N. and Peppas, L.B. 1996. Mechanical properties of hydrogels and their experimental determination. *Biomaterials* 17. 1647-1657
- Assink, R.A. **1977**. The study of domain structure in polyurethanes by nuclear magnetic resonance. *J. Polym. Sci., Polym. Phys. Ed.*15: 59.
- Badri, K.H., Othman, Z. and Ahmad, S.H. **2004**. Rigid polyurethane foams from oil palm resources. *J.Mater.Sci.* 39 ,5541-5542
- Bakare, I.O., Pavithran, C., Okieimen, F.E. and Pillai, C.K.S. **2006**. Polyesters from Renewable Resources: Preparation and Characterization. *Journal of Applied Polymer Science* 100: 3748-3755
- Baryeh, E.A. **2001**. Effects of Palm Oil Processing Parameter on Yield. *J.Food Eng.* 48 :1-6.

- Bhunia, H.P., Jana, R.N., Basak, A., Lenka, S. and Nando, B. **1998**. Synthesis of Polyurethane from Cashew Nut Shell Liquid (CNSL), a Renewable Resource, *Journal of Polymer Science: Part A: Polymer Chemistry* 36: 391–400
- Boczkowska, A and Gruin, I. **1999**. Polyurethanes from crystalline prepolymers *European Polymer Journal* 35:1569-1579
- Boguslavskii, D.B., Borodushkina, Kh. N. and Suvorova, Z.F. **1979**. Synthesis of poly (diene-urethanes) within diene elastomers. *Polymer Science U.S.S.R.*20: 1386-1392.
- Brown, M.E., Maciejewski, M., Vyazovkin, S., Nomen, R., Sempere, J., Burnhame, A., Opfermann, J., Strey, R., Anderson, H.L., Kemmler, A., Keuleers, R., Janssens, J., Desseyn, H.O., Lii, C.R., Tang, T.B., Roduit, B., Malek, J. and Mitsuhashi, T. **2000**. Computational aspects of kinetic analysis Part A: The ICTAC kinetics project-data, methods and results. *Thermochimica Acta* 355 : 125-143
- Bushfield, W.K. **1982**. Dynamic mechanical properties of some polycaprolactone based, crosslinked, crystallizable polyurethanes”, *J. Maeromolec. Sci. Chem.*, A17: 297
- Camberlin, Y and Pascault, J.P. **1983**. Phase segregation kinetics in segmented linear polyurethanes: Relations between equilibrium time and chain mobility and between equilibrium degree of segregation and interaction parameter. *J. Polym. Sci., Polym. Chem. Ed.* 22: 1835
- Camberlin, Y and Pascault, J.P. **1983**. Quantitative DSC evaluation of phase segregation rate in linear polyurethanes and polyurethaneureas. *J. Polym. Sci., Polym. Chem. Ed.* 21: 415.
- Chang, J.H. and Park, D.K. **2001**. Nanocomposites of Poly(ethylene terephthalate-co-ethylene naphthalate) with Organoclay. *Journal of Polymer Science: Part B: Polymer Physics* 39: 2581–2588
- Chang, J.H., An, Y.U., Ryu, S.C. and Giannelis, E.P. **2003**. Synthesis of Poly (butylene terephthalate) Nanocomposite by *In situ* Interlayer Polymerization and Characterization of Its Fiber (I). *Polymer Bulletin* 51: 69-75
- Chen Tsai, C.H.Y., Thomas, E.L., Macknight, W.J. and Schneider, N.S. **1986**. Structure and morphology of segmented polyurethanes. 3. Electron microscopy and small angle X-ray scattering studies of amorphous random segmented polyurethanes. *Polymer* 27: 659.
- Chen, T.K., Tien, Y.I. and Wei, K.H. **1999**. Synthesis and characterization of novel segmented polyurethane/clay nanocomposite via poly (ϵ -caprolactone)/clay. *Journal of Polymer Science: Part A: Polymer Chemistry* 37: 2225-2233
- Chen, T.K., Tien, Y.I. and Wei, K.H. **2000**. Synthesis and characterization of novel segmented polyurethane/clay

- nanocomposites. *Polymer* 41: 1345-1353
- Chen, G., Ma, Y. and Qi, Z. **2001** Preparation and morphological study of an exfoliated polystyrene/montmorillonite nanocomposites. *Scripta Materialia* 44 (1) 125-128.
- Chen, Y., Zhou, S., Yang, H., Gu, G. and Wu, L. **2004**. Preparation and characterization of nanocomposite polyurethane. *Journal of Colloid and Interface Science* 279 : 370-378
- Chen, Y., Zhou, S., Gu, G. and Wu, L. **2006**. Microstructure and properties of polyester-based polyurethane/titania hybrid films prepared by sol-gel process *Polymer* 47 : 1640-1648
- Choi, W.J., Kim, S.H., Kim, Y.J. and Kim, S.C. **2004**. Synthesis of chain-extended organifier and properties of polyurethane/clay nanocomposites. *Polymer* 45: 6045-6057
- Czech, P., Okrasa, L., Boiteux, G., Mechin, F. and Ulanski, J. **2005**. Polyurethane networks based on hyperbranched polyesters: Synthesis and molecular relaxations. *Journal of Non-Crystalline Solids* 351: 2735-2741.
- Czech, P., Okrasa, L., Me´chin, F., Boiteux, g.and Ulanski, J. **2006**. Investigation of the polyurethane chain length influence on the molecular dynamics in networks crosslinked by hyperbranched polyester. *Polymer* 47. 7207-7215
- Chun, B.C., Cho, T.K., Chung, Y.C. **2006**. Enhanced mechanical and shape memory properties of polyurethane block copolymers chain-extended by ethylene diamines. *European Polymer Journal* 42 : 3367-3373
- Dai, X., Xu, J., Guo, X., Lu, Y., Shen, D., Zhao, N., Luo, X. and Zhang, X., **2004**. Study on Structure and Orientation Action of Polyurethane Nanocomposites. *Macromolecules* 37, 5615.
- Dickie, R.A. **1979** “Mechanical properties (small deformations) of multiphase polymer blends, Polymer Blends”, Chap. 8, Vol. I (D. R. PAUL and S. NEWMAN Eds), Academic Press, New York.
- Delides, C and Pethrick, R.A. **1982**. Ultrasonic and dielectric studies of segmented polyurethanes. *Eur. Polym. J.* 17: 675.
- Duquesne, S., Jama, C., Le Bras, M., Delobel, R., Recourt, P. and Gloaguen, J.M.. **2003**. Elaboration of EVA-nanoclay systems—characterization, thermal behaviour and fire performance. *Composite Science and Technology* 63 : 114
- Edwards K.N (ed).**1981**. Urethane Chemistry and Applications, pp. 80-114. American Chemical Society. Washington, D.C., U.S.A
- Eychenne, V. and Mouloungui, Z. **1999**. High concentration of 1-(3-)monoglycerides by direct partial esterification of fatty acids with glycerol. *Fett/Lipid* 101 : 424-427
- Falkes, M.T (ed), “Processing, Structure and Properties of Block Copolymer”, pp. 25-78. Elsevier Publisher, 1955, London.
- Fisher, H.R., Gielgens, L.H. and Koster, T.P.M. **1999**. Nanocomposites

- from polymers and layered materials. *Acta Polym.* 50 : 122-126
- Fu, X and Qutubuddin, S. **2001**. Polymer-clay nanocomposites: exfoliation of organophilic montmorillonite nanolayers in polystyrene. *Polymer* 42 : 807-813
- Fornes, T.D. and Paul, D.R. **2003**. Modeling properties of nylon 6/clay nanocomposites using composites theories. *Polymer* 44 : 4993
- Gertzmann, R and Gurtler, C. **2005**. A catalyst system for the formation of amides by reaction of carboxylic acids with blocked isocyanates. *Tetrahedron Letters* 46 : 6659–6662
- Giannelis, E.P. 1996. Polymer layered silicate nanocomposite. *Advanced Materials* 8: 29-35
- Gilman, J.W. **1999**. Flammability and thermal stability studies of polymer layered-silicate (clay) nanocomposites. *Applied clay science* 15 : 31-49.
- Gopakumar, S. and Gopinathan Nair, M.R. **2006**. Solution properties of NR/PU block copolymer by size-exclusion chromatography and viscometry. *Journal of Polymer Science : Part B : Polymer Physics* 44 : 2104-2111
- Gorrasi, G., Tortora M. and Vittoris, V. **2005**. Synthesis and Physical Properties of Layered Silicates/ Polyurethane Nanocomposites. *Journal of Polymer Science: Part B: Polymer Physics* 43. 2454
- Gorasi, G., Tortora, M., Vittoria, V., Pollet, E., Lepoittevin, B., Alexandre, M. and Dubois, P. **2003**. Vapour barrier properties of polycaprolactone montmorillonite nanocomposites: effect of clay dispersion. *Polymer* 44 : 2271-2279.
- Gu, A. and Liang, G. **2003**. Thermal degradation behaviour and kinetic analysis of epoxy/montmorillonite nanocomposites. *Polymer Degradation and Stability* 80 : 383-391.
- Guo, A., Demydov, D., Zhang, W. and Petrovic, Z.S. **2002**. Polyols and Polyurethanes from Hydroformylation of Soybean Oil “, *Journal of Polymers and the Environment* 10: 49-52.
- Hashimoto, T., Todo, A., Itoi, H. and Kawai, H. **1977**. Domain-boundary structure of styrene isoprene block copolymer films cast from solutions. 2. Quantitative estimation of the interfacial thickness of lamellar microphase systems. *Macromolecules* 10: 377-384
- Hamilton, R.J. (ed). **1995**. Developments in oils and fats”, pp.32-55. Chapman & Hall, Great Britain
- Heal, G.R. **2005**. A generalization of the non-parametric, NPK(SVD) kinetic method Part 1. Isothermal experiment. *Thermochimica Acta* 426: 15-21
- Hilmi Mahmood, M. **1987**. The formation and properties of segmented polyurethane elastomers. Nuclear Energy Unit-Prime Minister’s Department. Malaysia.
- Hilmi Mahmood, M (patent application), “Method For Manufacturing Palm Oil Based Hydroxyl Containing Products For Use In Making Polyurethane Materials”, No fail

- Horgnies, M. and Ceretti, E.D. **2006**. Study of siloxane additives migration to the surface of polyester-(melamine)-polyurethane coatings: Aging effects after ethanol cleaning. *Progress in Organic Coatings* 55 : 27–34
- Howard, G.T. **2002**. Biodegradation of polyurethane: a review. *International Biodeterioration & Biodegradation* 49: 245 – 252
- Hsueh, C.H. **2000**. Young's modulus of unidirectional discontinuous - fibre composites. *Composites Science and Technology* 60 . 2671
- Hu, Y., Song, L., Xu, J., Yang, L., Chen, Z. and Fan, W. **2001**. Synthesis of polyurethane/clay intercalated nanocomposites. *Colloid Polym. Sci.*, 279: 819-822
- Hussain, M. and Simon, G.P. **2003**. Fabrication of phosphorus-clay polymer nanocomposites for fire performance. *Journal of materials Science Letters* 22: 1471-1475
- Jayaraman, K. **2003**. Manufacturing sisal-propylene composite with minimum fiber degradation. *Journal of Composite Science and Technology* 63: 116
- Jia, Q.M., Zheng, M., Zhu, Y.C., Li, J.B. and Xu, C.Z. **2007**. Effects of organophilic montmorillonite on hydrogen bonding, free volume and glass transition temperature of epoxy resin/polyurethane interpenetrating polymer networks. *European polymer journal* 43, 35
- Jiang, X., Li, J., Ding, M., Tan, H., Liang, Q., Zhong, Y., Fu, Q. **2007**. Synthesis and degradation of nontoxic biodegradable waterborne polyurethanes elastomer with poly(ϵ -caprolactone) and poly(ethylene glycol) as soft segment. *European Polymer Journal*.
- Kato, M. and Usuki, A. **2000**. Polymer-clay nanocomposites. In *Polymer-clay nanocomposites*, ed. Pinnavaia, T.J. and Baell, G.W. pp 97-109. England : John Wiley & Sons, Ltd.
- Kashiwagi, T., Harris Jr., R.H., Zhang, X., Briber, R.M., Cipriano, B.H., Raghavan, S.R., Awad, W.H. and Shields, J.R. **2004**. Flame retardant mechanism of polyamide 6–clay nanocomposites. *Polymer* 45: 881–891
- Koberstein, J.T and Stein, R.S. **1983**. Small-angle X-ray scattering measurements of diffuse phase boundary thickness in segmented polyurethane elastomers. *J. Polym. Sci., Polym. Phys. Ed.* 21: 2181
- Koberstein, J.T. and Stein, R.S. **1984**. Small-angle light scattering studies of macrophase separation in segmented polyurethane block copolymers. *Polymer* 25: 171.
- Kodera, Y. and McCoy, B.J. **2002**. Distribution kinetics of polymer thermogravimetric analysis : A model for chain-end and random scission. *Energy & Fuels* 16 : 119-126.
- Kojima, Y., Usuki, A., Kawasumi, M., Okada, A., Fukushima, Y., Kurauchi, T., Kamigato, O. **1993**. Mechanical properties of Nylon 6-Clay Hybrid. *Journal of material Research* 8: 1185
- Kojio, K., Nakamura, S. and Furukawa, M. **2004**. Effect of side methyl groups

- of polymer glycol on elongation induced crystallization behaviour of polyurethane elastomers. *Polymer* 45 : 8147-8155.
- Kornmann, X., Lindberg, H. and Berglund, L.A. **2001**. Synthesis of epoxy-clay nanocomposites: influence of the nature of the clay on structure. *Polymer* 42: 1303–1310.
- Krol, P. and Pitera, B.P. **2003**. A study on the synthesis of urethane oligomers. *European Polymer Journal* 39 : 1229–1241
- Krol, P. **2007**. Synthesis methods, chemical structures and phase structures of linear polyurethanes. Properties and applications of linear polyurethanes in polyurethane elastomers, copolymers and ionomers. *Progress in Materials Science* 52 : 915-1015
- Krone, C.A. and Klingner, T.D. **2005**. Isocyanates, polyurethane and childhood asthma. *Pediatr Allergy Immunol* 16: 368–379
- Kuan, H.C., Chuang, W.P., Ma, C.C.M., Chiang, C.L. and Wu, H.L. **2005** Synthesis and characterization of a clay/waterborne polyurethane nanocomposite. *Journal of material science* 40: 179-185
- Lam, C.K., Cheung, H.Y., Lau, K.T., Zhou, L.M., Ho, M.W. and Hui, D. **2005**. Cluster size effect in hardness of nanoclay/epoxy composites. *Composites Part B: Engineering* 36. 263
- Lan, T. and Pinnavaia, T.J. **1994**. Clay-Reinforced Epoxy Nanocomposites. *Chem. Mater.* 6: 2216-2219
- Lagaly, G. **1986**. Interaction of alkylamines with different types of layered compounds. *Solid State Ionics* 22 : 43-51
- Latere Dwan'isa, J.P., Mohanty, A.K., Misra, M., Drzal, L.T. and Kazemizadeh, M. **2004**. Biobased polyurethane and its composite with glass fiber. *Journal of materials science* 39: 2081-2087
- Luda, M.P., Costa, L., Bracco, P. and Levchik, S.V. **2004**. Relevant factors in scorch generation in fire retarded flexible polyurethane foams II Reactivity of isocyanate, urea and urethane groups. *Polymer Degradation and Stability* 86 : 43-50
- LeBaron, P.C., Wang, Z. and Pinnavaia, T.J. **1999**. Polymer-layered silicate nanocomposites: an overview. *Applied Clay Science* 15: 11–29
- Lee, H.S., Wang, Y.K., Macknight, W.J. and Hsu, S.L. **1988**. Spectroscopic analysis of phase-separation kinetics in model polyurethanes. *Macromolecules*, 1988, 21, 270-273.
- Lee, H.S., Wang, Y.K. and Hsu, S.L. **1987**. Spectroscopic analysis of phase separation behavior of model polyurethanes. *Macromolecules* 20: 2089-2095.
- Lee, J. and Giannelis, E. **1997**. *Polymer Preprints* 38 : 688–689
- Lee, J., Takekoshi, T. and Giannelis, E., **1997**. *Mater. Res. Soc. Symp. Proc.* 457 : 513–518
- Lepoittevin, B., Devalckenaere, M., Pantourstier, N., Alexandre, M., Kubies, D., Calberg, C., Jerome, R. and Dubois, P. **2002**. Poly (ϵ -caprolactone)/clay

- nanocomposites prepared by melt intercalation: mechanical, thermal and rheological properties. *Polymer* 43: 4017 – 4023
- Lindermeir, E. and Tank, V. **1994**. The spectral emissivity of natural surfaces measured with a Fourier transform infrared spectrometer. *Measurement* 14. 177-187
- Lu, Y., Tighzert, L., Dol, P. and Erre, D. **2005**. Preparation and properties of starch thermoplastics modified with waterborne polyurethane from renewable resources”, *Polymer* 46: 9863-9870
- Markusch, P.H and Schmelzer, H.G. **1997**. Synthesis of Polyurethane Elastomers, Presented at a meeting of the Rubber Division, American Chemical Society. Anaheim, California
- Masiulanic, B., Hrouz, J., Baldrian, J., Ilavsky, M. and Dusek, K. **1987**. Dynamic mechanic behavior and structure of polyurethaneimides”, *J. Appl. Polym. Sci.*, 34: 1941.
- Maxwell, R.S., Chambers, D., Balazs, B., Cohenours, R. and Sung, W. **2003**. NMR analysis of γ -radiation induced degradation of halothane-88 polyurethane elastomers. *Polymer Degradation and Stability* 82 : 193-196
- Mecking, S. **2004**. Nature or Petrochemistry?—Biologically Degradable Materials. *Angew. Chem. Int. Ed.* 43 : 1078 –1085
- Mohan, T.P., Kumar, M.R. and Velmurugan, R. **2006**. Thermal, mechanical and vibration characteristics of epoxy-clay nanocomposites. *J Mater Sci* 41:5915–5925
- Nam, P.H., Maiti, P., Okamoto, M., Kotaka, T., Hasegawa, N. and Usuki, A. **2001**. A hierarchical structure and properties of intercalated polypropylene/clay nanocomposites. *Polymer* 42: 9633–40
- Nasar, A.S., Jikei, M. and Kakimoto, M. **2003**. Synthesis and properties of polyurethane elastomers crosslinked with amine-terminated AB₂-type hyperbranched polyamides. *European Polymer Journal* 39 : 1201
- Neumueller, W. and Bonart, R. 1982. Investigation of domain structure in segmented polyurethanes by means of small-angle X-ray scattering. *J. Macromolec. Sci. Phys.* B21: 203
- Nunes, R.C.R, Foncesa, J.L.C. and Pereira, M.R. **2000**. Polymer-filler interactions and mechanical properties of polyurethane elastomers. *Polymer Testing* 19: 93-103
- O’Brien, R.D. **2004**. Fats and Oil Formulating and processing for applications. Second edition. CRC Press. USA .
- Ogunniyi, D.S. **2006**. Castor oil: A vital industrial raw material. *Bioresource Technology* 97: 1086-1091
- Oertel, G. (Editor). **1985**. Polyurethane handbook, pp. 5-17. Hanser Publishers. Munich
- Oprea, S., Vlad, S. and Stanciu, A. **2001**. Poly(urethane-methacrylate)s. Synthesis and characterization. *Polymer* 42 :7257-7266

- Oprea, S. and Oprea, V. 2002. Mechanical behavior during different weathering test of the polyurethane elastomers film. *European Polymer Journal* 38 : 1205-1210
- Ortyl, E., Kucharski, S., and Gotszalk, T. **2005**. Refractive index modulation in the polyurethane films containing diazo sulfonamide chromophores. *Thin Solid Films* 479 : 288– 296
- Pattanayak, A. and Jana, S.C. **2005a**. Synthesis of thermoplastic polyurethane nanocomposites of reactive nanoclay by bulk polymerization methods. *Polymer* 46: 3275-3288
- Pattanayak, A. and Jana, S.C. **2005b**. Thermoplastic polyurethane nanocomposites of reactive silicate clays: effects of soft segments on properties. *Polymer* 46:5183
- Park, H.B., Kim, C.K. and Lee, Y.K. **2002**. Gas separation properties of polysiloxane/polyether mixed soft segment urethane urea membranes. *Journal of Membrane Science* 15: 257
- Pasch, H. and Trathnigg, B. 1998. HPLC of Polymer, pp 41. Berlin: Springer
- Paul, C., Gopanathan Nair, M.R., Neelakantan, N.R., Koshy, P., Idage, B.B. and Bhelhekar, A.A. **1998**. Segmented block copolymers of natural rubber and 1.3-butanediol-toluene diisocyanate digomers. *Polymer* 39: 6861
- Peterson, D.J., Vyazovkin, S. and Wight, C.A. **1999**. Kinetic study of stabilizing effect of oxygen on thermal degradation of Poly(methyl metacrylate). *J.Phys.Chem. B.* 103 : 8087-8092
- Petrovic, Z.S and Ferguson, J. **1991**. Polyurethane Elastomers. *Progress in Polymer Science* 16: 695-836.
- Pinto, V.A., Visconte Yuan, L.L. and Reis Nunes, R.C. **2001**. Mechanical properties of thermoplastic polyurethane elastomer with mica and aluminum trihydrate. *European Polymer Journal* 37: 1935-1937
- Prisacariu, C., Olley, R.H., Caraculacu, A.A., Bassett, D.C. and Martin, C. **2003**. The effect of hard segment ordering in copolyurethane elastomers obtained by using simultaneously two types of diisocyanates. *Polymer* 44 : 5407-5421
- Ray, S.S., Maiti, P., Okamoto, M., Yamada, K. and Ueda, K. **2002**. New Poly(lactide/Layered Silicate Nanocomposites. 1. Preparation, Characterization, and Properties. *Macromolecules* 35: 3104-3110
- Ray, S.S. and Okamoto, M. **2003**. Polymer/layered silicate nanocomposites: a review from preparation to processing. *Progress in polymer science* 28: 1539-1641
- Rekondo, A., Fernandez-Berridi, M.J. and Irusta, L **2006**. Synthesis of silanized polyether urethane hybrid systems. Study of the curing process through hydrogen bonding interactions. *European Polymer Journal* 42. 2069
- Redlich, C.A. and Karol, M.H. **2002**. Diisocyanate asthma: clinical aspects and immunopathogenesis.

- International
Immunopharmacology 2, 213-224
- Rihayat, T., Saari, M., Hilmi Mahmood, M., Wan Yunus, W.M.Z., Suraya, A.R., Dahlan, K.Z.H.M. and Sapuan, S.M. **2007**. Mechanical Characterisation of Polyurethane/Clay Nanocomposites. *Polymers & Polymer Composites* 15: 597-602
- Rogulska, M., Podkomcielny, W., Kultys, A., Pikus, S. and Posdzik, E. **2006**. Studies on thermoplastic polyurethanes based on new diphenylethane-derivative diols. I. Synthesis and characterization of nonsegmented polyurethanes from HDI and MDI. *European Polymer Journal* 42: 1786-1797
- Romero, G. and Sanchez (Eds.). **2004** Functional Hybrid Materials. Wiley-VCH. Weinheim.
- Salunkhe, D.K., Chavan, J.K., Adsule, R.N. and Kadam, S.S. **1992**. World oilseeds chemistry, technology, and utilization. An avi Book Published by Van Nostrand Reinhold. New York. pp. 512-515
- Sanchez-Adsuar, M.S. **2000**. Influence of the composition on the crystallinity and adhesion properties of thermoplastic polyurethane elastomers. *International Journal of Adhesion and Adhesives* 20 : 291-298
- Serrano, M., Macknight, W.J., Thomas, E.L. and Ottino, J.M. **1987**. Transport-morphology relationships in segmented polybutadiene polyurethanes: 1. Experimental result. *Polymer* 28: 1667
- Sheth, J.P., Wilkes, G.L., Fornof, A.R., Long, T.L. and Yilgor, I. **2005**. Probing the hard segment phase connectivity and percolation in model segmented poly(urethane urea) copolymers. *Macromolecules* 38: 5681
- Serrano, M., Macknight, W.J., Thomas, E.L. and Ottino, J.M. **1987**. Transport-morphology relationships in segmented polybutadiene polyurethanes: 1. Experimental results. *Polymer* 28: 1667.
- Silva Araújo, R.C and Duarte Pasa, V.M. **2004**. New Eucalyptus tar-derived polyurethane coatings. *Progress in Organic Coating* 51: 6-14
- Song, M., Xia, H.S., Yao, K.J. and Hourston, D.J. **2005a**. A study on phase morphology and surface properties of polyurethane/organoclay nanocomposite. *Eur. Polym. J.* 41, 259-266 (1)
- Song, L., Hu, Y., Tang, Y., Zhang, R., Chen, Z. and Fan, W. **2005b**. Study on the properties of flame retardant polyurethane/organoclay nanocomposites. *Polymer Degradation and Stability* 87 : 111-116.
- Suresh, K.I. and Kishanprasad, V.S. **2005**. Synthesis, structure, and properties of novel polyol from cardanol and developed polyurethanes. *Ind.Eng.Chem.Res.* 44 : 4504-4512
- Suhara, F., Kutty, S.K.N. and Nando, G.B. **1998**. Thermal degradation of short polyester fiber-polyurethane elastomer composite. *Polymer Degradation and Stability* 61 : 9-13
- Tang, Z., Maroto Valer, M.M., Andresen, J.M., Miller, J.W., Listemenn, M.L., McDaniel, P.L., Morita,

- D.K. and Furlan, W.R. **2002**. Thermal degradation behavior of rigid polyurethane foams prepared with different fire retardant concentrations and blowing agents. *Polymer* 43: 6471-6479.
- Tien, Y.I and Wei, K.H. **2001**. Hydrogen bonding and mechanical properties on segmented montmorillonite/polyurethane nanocomposites of different hard segment ratios”, *Polymer* 42 : 3213-3221.
- Thiele, L. **1979**. Isocyanatreaktionen und Katalyse in der Polyurethanchemie Fortschrittsbericht. *Acta Polymerica* 30: 323-342
- Theocaris, P.C and Varias, A.G. **1985**. Thermal expansion properties of particulates based on the concept of mesophase. *J. Appl. Polym. Sci.*30: 2979-2995
- Tsujimoto, T., Uyama, H. and Kobayashi, S. **2004**. Synthesis and Curing Behaviors of Cross-Linkable Polynaphthols from Renewable Resources: Preparation of Artificial Urushi”, *Macromolecules* 37: 1777-1782
- Tortora, M., Gorrasi, G., Vittoria, V., Galli, G., Ritrovati, S. and Chiellini, E. **2002**. Structural characterization and transport properties of organically modified montmorillonite/polyurethane nanocomposites. *Polymer* 43: 6147–6157.
- Tundo, P., Anastas, P., Black, D.S., Breen, J., Collins, T., Memoli, S., Miyamoto, J., Polyakoff, M. and Tumas, W., **2000**. Synthetic pathways and processes in green chemistry : Introductory overview. *Pure Appl. Chem.*72 : 1207–1228
- Tyan, H.L., Wei, K.H. and Hsieh, T.E. **2000**. Mechanical Properties of Clay–Polyimide (BTDA–ODA) Nanocomposites via ODA-Modified Organoclay. *Journal of Polymer Science: Part B: Polymer Physics*38: 2873–2878
- Tyan, H. L., Liu, Y.C. and Wei, K.H. **1999**. Thermally and Mechanically Enhanced Clay/Polyimide Nanocomposite via Reactive Organoclay. *Chem. Mater.* 11: 1942-1947
- Urquhart, S.G., Smith, A.P., Ade, H.W., Hithcock, A.P., Rightor, A.G. and Lidy, W. **1999**. Near-Edge X-Ray Absorption Fine Structure Spectroscopy of MDI and TDI Polyurethane Polymers. *J. Phys.Chem. B* 103: 4603
- Usuki, A., Kojima, Y., Kawasumi, Okada, A., Fukushima, Y., Kurauchi, T. and Kamigaito, O. **1993**. “Synthesis of nylon 6-clay hybrid”, *Journal of Materials Resesarch* 8 : 1179-1185
- Usuki, A; Kato, M; Okada, A; Kurauchi, T. 1997. Synthesis of polypropylene-clay hybrid. *Journal of applied polymer science* 63 : 137
- Utracki, L.A. **2004**. Clay-Containing Polymeric Nanocomposites. Vol.1.Rapra Technology Limited. United Kingdom. pp.1-30
- Uyama, H., Kuwabara, M., Tsujimoto, T., Nakano, M., Usuki, A. and Kobayashi, S. **2003**. Green Nanocomposites from Renewable Resources: Plant Oil-Clay Hybrid Materials. *Chemistry of Materials* 15: 2492-2494
- Vaia, R.A., Teukolsky, R.K. and Giannelis, E.P. **1994**. Interlayer Structure and

- Molecular Environment of Alkylammonium Layered Silicates. *Chem. Mater.*; 1017-1022.
- Valence, M.A., Yeung, S.A and Cooper, S.L. **1983**. A dielectric study of the glass transition region in segmented polyether-urethane copolymers. *Colloid Polym. Sci.*, 261: 541.
- Varlot, K.M., Reynaud, E., Vigier, G. and Varlet, J., **2002**. Mechanical Properties of Clay-Reinforced Polyamide. *Journal of Polymer Science: Part B: Polymer Physics* 40: 272–283
- Voznyakovskii, A.P., Genkin, A.P., Plyushch, A.V. and Petrova, N.A. **1986**. “Method of contrastation of samples of block copolymers containing the rigid block to study their domain structure by electron microscopy method. *Vysokomol. Soyed., Ser. A* 28: 2621.
- Vyazovkin, S., Dranca, I., Fan, X. and Advincula, R. **2004**. Degradation and relaxation kinetics of polystyrene-clay nanocomposites prepared by surface initiated polymerization. *J.Phys.Chem.* 108 : 11672-11679
- Wambua, P., Ivens, J. and Verpoest, I. **2003**. Natural fibers: can they replace glass in fiber reinforced plastics?. *Journal of Composite Science and Technology* 63: 1259
- Wang, K., Chen, L., Wu, J., Toh, M.L., He, C. and Yee, A.F. **2005**. Epoxy Nanocomposites with Highly Exfoliated Clay: Mechanical Properties and Fracture Mechanisms. *Macromolecules* 38: 788-800
- Wang, K., Chen, L., Kotaki, M. and He. C. **2007**. Preparation, microstructure and thermal mechanical properties of epoxy/crude clay nanocomposites. *Composites: Part A* 38 : 192-197
- Wang, K.H., Choi, M.H., Koo, C.H., Choi, Y.S. and Chung, I.J. **2001**. Synthesis and characterization of maleated polyethylene/clay nanocomposites. *Polymer* 42 : 9819-9826
- Wang, S., Hu, Y., Song, L., Wang, Z., Chen, Z. and Fan, W. **2002**. Preparation and thermal properties of ABS/montmorillonite Nanocomposites. *Polymer Degradation and Stability* 77: 423-426
- Wang, X. and Luo, X. **2004**. A polymer network based on thermoplastic polyurethane and ethylene-propylene-diene elastomer via melt blending: morphology, mechanical properties, and rheology. *European Polymer Journal* 40 : 2391
- Wang, Z. and Pinnavaia, T.J. **1998**. Nanolayer Reinforcement of Elastomeric Polyurethane. *Chem. Mater.*10: 3769-3771
- Warwel, S., Bruse, F., Demes, C., Kunz, M, and Klaas, M.R. **2001**. Polymers and surfactants on the basis of renewable resources. *Chemosphere* 43: 39-48
- Wegener, G., Brandt, M., Duda, L., Hofmann, J., Kleczewski, B., Koch, D., Kumpf, R.J., Orzesek, H., Pirkl, H.G., Six, C., Steinlein, C. and Weisbeck, M. **2001**. Trends in industrial catalysis in the polyurethane industry. *Applied*

- Catalysis A: General* 221: 303-335.
- Wicks, A.D. and Wicks Jr, W.Z. **1999**. Blocked isocyanates III: Part A. Mechanisms and chemistry. *Progress in Organic Coatings* 36 :148-172
- Wicks, A.D. and Wicks Jr, W.Z. **2001**. Blocked isocyanates III: Part B. Uses and applications of blocked isocyanates. *J. Progress in Organic Coatings* 41 : 1–83
- Wirpsza, Z. **1993**. Polyurethanes Chemistry, Technology and Application, pp. 1-60. Ellis Horwood Limited Publisher. Chichester, British.
- Wu, Q., Xue, Z., Qi, Z. and Wang, F. **2000**. Synthesis and characterization of PAN/clay nanocomposite with extended chain conformation of polyaniline. *Polymer* 41: 2029-2032.
- Xiong, J., Liu, Y., Yang, X. and Wang, X. **2004**. Thermal and mechanical properties of polyurethane/montmorillonite nanocomposites based on a novel reactive modifier. *Polym. Degrad. Stab.* 86, 549
- Xie, H.Q. and Guo, J.S. **2002**. Room temperature synthesis and mechanical properties of two kinds of elastomeric interpenetrating polymer networks based on castor oil. *European Polymer Journal* 38 : 2271
- Yano, K., Usuki, A., Okada, A., Kurauchi, T. and Kamigaito, O. **1993**. Synthesis and properties of polyimide clay hybrid. *Journal of Polymer Science: Part A : Polymer Chemistry* 31: 2493-2498
- Yeganeh, H. and Mehdizadeh, M.R. **2004**. Synthesis and properties of isocyanate curable millable polyurethane elastomers based on castor oil as a renewable resource polyol. *European Polymer Journal* 40: 1233-1238
- Yusoff, S. **2006**. Renewable energy from palm oil - innovation on effective utilization of waste. *Journal of Cleaner Production* 14: 87-93
- Zhao, C., Qin, H., Gong, F., Feng, M., Zhang, S. and Yang, M. **2005a**. Mechanical, thermal and flammability properties of polyethylene/clay nanocomposites. *Polymer Degradation and Stability* 87 : 183-189
- Zhou, Y., Rangari, V., Mahfuza, H., Jeelani, S. and Mallick, P.K. **2005b**. Experimental study on thermal and mechanical behavior of polypropylene, talc/polypropylene and polypropylene/clay nanocomposites. *Materials Science and Engineering A* 402:109–117